Fabrication and Characterization of MOF and Stearic Acid Based Biomimetic Sponges for Efficient Oil/Water Separation

By

Tasmia Azam

School of Chemical and Materials Engineering

National University of Sciences and Technology

2020

Fabrication and Characterization of MOF and Stearic Acid Based Biomimetic Sponges Efficient Oil/Water Separation

Name: Tasmia Azam

Reg. No: 00000204391

This thesis is submitted as a partial fulfillment of the requirement for the degree of

MS in Chemical Engineering

Supervisor: Dr. Erum Pervaiz

School of Chemical and Materials Engineering (SCME)

National University of Sciences and Technology (NUST)

H-12 Islamabad, Pakistan

June, 2020

DEDICATION

This thesis is dedicated to my beloved parents, Muhammad Azam and Kousar Nasreen, for nursing me with love and affection, whose endless support and encouragement set the foundation for the discipline and inspiration required to accomplish this work.

Acknowledgements

In the name of **Allah**, The Most Beneficent and The Most Benignant. All admirations to **Almighty Allah**, the administration of knowledge and instigator of resources, abilities and opportunities. It is the strength of His love that supplied me with the courage and the guidance to complete this research work.

First of all, I pay my sincerest recognition to my supervisor, **Dr. Erum Pervaiz** Associate Professor, SCME NUST. Her guidance, unconditional support, and confidence in me made this task attainable. I am thankful to her for making me to think outside the box and do something different. It was not possible to finish my research without her supervision.

Secondly, I want to offer my appreciation to the Principal, SCME NUST, **Dr. Zakir Hussain** and Head of Department, SCME NUST, **Dr. Muhammad Bilal Khan Niazi** for providing me with an excellent atmosphere to accomplish my research work. I want to thank my GEC members **Dr. Sarah Farrukh** (SCME NUST) **Dr. Tayyaba Noor** (SCME, NUST) for their continuous assistance and recommendations. I want to pay my special Thanks to **Dr. Sofia Javed** (SCME, NUST) for providing her lab the facility of contact angles measurement.

Words are not enough to express my heartiest gratitude to my **parents**, my **grandparents** and my **sisters** for providing me with endless support and continuous motivation throughout my educational career and during the process of my research and writing this thesis. This would not have been achievable without their immeasurable support and love. I am honored and blessed to have them in my life.

Finally yet importantly, I am highly thankful to my wonderful friends especially **Misbah Iqbal**, **Mayra Akhtar, Rimal Raza and Amber Saleem** for their much needed encouragement, love, affectionate attitude and joyous company during my stay at the university. At the end, my deepest appreciation to each and every person, who in one way or another contributed in the completion of my thesis. May Allah Almighty bless all of you!

Tasmia Azam

Abstract

Fabrication of highly hydrophobic surfaces by bio mimicking the 'Lotus Effect' is turning out to be an area of active research in the field of oil/water separation. Current work is related to the fabrication of MOF functionalized, stearic acid functionalized and composite, incorporating MOF and stearic acid, functionalized biomimetic hydrophobic sponges by utilizing the inherited properties of MOFs i.e. large surface area, controllable pore size and chemical functionality at molecular level, non-wetting property of stearic acid and regular 3D skeleton of highly porous polyurethane sponge. The effect of loading of functionalizing agents on hydrophobicity of the sponge is studied by changing the concentration of reactants. The prepared sponges were analyzed by x-ray diffraction, scanning electron microscopy, fourier transmission infrared spectroscopy and sessile drop technique to conform the prerequisites of lotus effect. It is found that a continuous and uniform layer of ZIF-8 on sponge skeleton forms by using a molar ratio 1:8.08: 124.93 of Zn^{+2}, Hmim and MeOH respectively, giving highest hydrophobicity (WCA=129.2°) among MOF functionalized sponges while in stearic acid functionalized sponges and in composite functionalized sponges hydrophobicity decreases by increasing the concentration of stearic acid. MOF functionalized sponge with continuous layer of ZIF-8 showed comparatively good absorption capacity ranging from 28 to 79 times its own weigh that is stable up to 10 absorption/desorption cycles. The composite i.e. stearic acid @ MOF, decorated on sponge template inherited all properties of its parent components showing high hydrophobicity (WCA=140.8°) and high absorption capacity that is constant for 10 absorption/desorption cycles for different oils/organic solvents ranging from 30.26 to 115.35 times its own weight. The method of fabrication is easy, economical and does not required any pre modification of sponge by surfactants. Moreover, the prepared sponges are easy to handle and absorbed oil can be recovered simply by manual squeezing.

Table of Contents

List of Figures

List of Tables

List of Abbreviation

PS	Pristine polyurethane sponge / Pristine sponge
MOF	Metal organic framework
ZIF-8	Zeolitic imidazolate framework
SA	Streaic acid
AC	Absorption capacity
CC	Collection capacity
x	Cycle number i.e. 1,2,3,4,……
AC_x	Absorption capacity of cycle x
CC_x	Collection capacity of cycle x
Rc	Recyclability
WCA	Water contact angle
OCA	Oil contact angle
ZIF-8 @ Sponge	Sponge coated with ZIF-8
SA @ Sponge	Sponge coated with stearic acid
SA @ ZIF-8 @ Sponge	Sponge coated with layers of ZIF-8 and stearic acid respectively
ZIF-8 @ SA @ Sponge	Sponge coated with layers of stearic acid and ZIF-8 respectively
SA @ SA @ZIF-8 @ Sponge	Sponge coated with layers of ZIF-8, stearic acid and stearic acid respectively

Chapter No. 01

Introduction

1.1. Background

Water is a vital and common need of life, directly or indirectly effecting life activities. Its importance is absolutely undeniable. Living organisms, industries, environment and metabolic processes all are water dependent. But due to increase in population and rapid industrialization water is contaminating everyday all over the world posing serious threats to environment, human and aquatic life as well. This is of serious concern as earth is becoming short of clean water with every passing year. Environmental sustainability which is directly apprehensive with the future of humanity, defines the ways to secure and control the sustainability of earth's resources like water quality, air quality and ecosystem. It also plays its part to avert the forthcoming damage because of technical advancement. In case of water, environmental sustainability can be achieved by efficient water treatment [1]. With increased water pollution the advancements in the field of water treatment are becoming exceptional. In context of problem of pollution in 1948 first major US law 'The Federal Water Pollution Control Act' was passed. In 1972 clean water act (CWA) was passed with primary focus to control point source pollution by 'using end of pipe' pollution control approach for factories and sewers [2]. A major breakthrough happened in the field of water treatment in 1850s when it was found that Cholera is water born disease. With passing centuries, from boiling, filtration by using charcoal and sand, exposing to sunlight for removing unwanted particles and bad smell from drinking water the water treatment methods have now reached to an advanced level of membrane separation and absorption through 3D porous nanoparticle absorbents.

1.2. Water Pollution

Water pollution is one of utmost concerns for environmentalists these days. It is defined as the condition when the concentration of harmful chemicals or microorganisms in water bodies such as ground water, oceans, rivers and lakes reaches to a point where it poses threats to aquatic as well as human life. Being a universal solvent water dissolves

almost everything in it that's why it can be easily contaminated as well. Surface water and ground water are considered to be most affected water bodies.

1.2.1. Types of Water Pollution

Surface water can be polluted by following three ways.

- Point source pollution
- No-point source pollution
- Transboundary pollution

When there is a single source of pollution or when the pollution in water body is coming from one point then this is called point source pollution from example effluent coming from drainage pipe of an industry and oil spill from a ship carrying oil tanker. When the source of pollution is not single but multiple sources are discharging effluent in a single water body then this is termed non-point source pollution. Transboundary pollution is situation when the pollution entering the water body at one point scatters to hundreds and thousands of miles away for example, radioactive waste from nuclear power station discharged to a nearby river [3].

1.2.2. Causes of Water Pollution

Water pollution does not start from within the water itself. Most of it comes from land from point and non-point sources. Water pollution can be caused by a number of reasons including domestic sewage, industrial waste water, and agricultural waste being discharged into a water body. Other reasons are acid rain global warming. Apart from that one other reason which particularly affects marine environment is oil spills accidents that cause oil pollution in water which is the main focus of this study. These all are responsible for discharge of many inorganic and organic pollutants in water [3].

1.3. Oil / water Pollution

Oil and Organics are common pollutants in waste water. Many industries e.g. food, mining, textile, leather cement, steel, pharmaceutical and petrochemical industry produce oily waste water. Table 1.1 lists the sources of oily waste from different industries while table 1.2 shows the oil and grease concentration in effluent of different factories. However in oceans and seas most significant forms of pollution is also oil/water pollution with adverse damages to marine ecosystems, assets and resources. Oil pollution in oceans and seas occurs because of following reasons (Figure 1).

1. Natural seeping of oil from oil reserves under oceans.
2. Problems in offshore drilling of oil
3. Leakage of oil from transportation pipes and takers transporting oils through ships
4. Runoff from land sources (Industries, machines and activities of modern economy) [4].

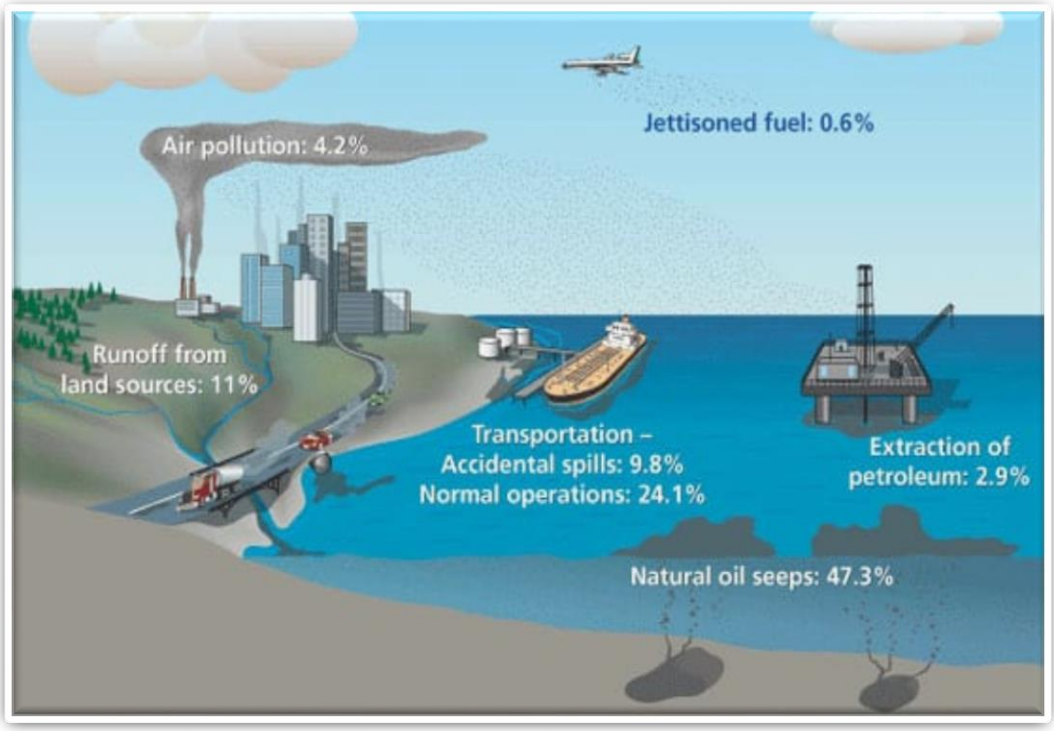

Figure 1. 1 Sources of oil / water pollution in oceans and seas

Table 1. 1 Sources of oily wastes from different industries

Source	Industries	Nature
Alkaline and acid cleaners	Metal fabrication, iron and steel, metal finishing, industrial laundries	High emulsified because of presence surfactants, hard to treat.
Floor washes	All industries	Mixture of different types of oil, dirt, debris and solvents. Can be emulsified and free.
Machine coolant	Metals manufacturing machining	Emulsified hard to treat.
Vegetable and animal fats splitting, refining, rendering	Edible oil, detergent manufacturing, fish processing, textile (wool scouring), tank car washing,	Can be emulsified and free. Treatment difficulty varies from easy to hard.
Petroleum oils	Petroleum refining, petroleum drilling	Can be emulsified and free. Treatment difficulty varies from easy to hard.

Adapted from Cheryan and Rajagopolan [5].

Table 1. 2 Oil and grease concentration in waste water of selected industries

Type of Industry	Oil and Grease Concentration(mg/L)
Palm oil Industry	4000
Food Processing	3000-4000
Mining operation	3000-23,000
Metal finishing	100-5,000
Steel-rolling mill	7200
Aluminum rolling	5000-50,000
Oil drilling	7-1300
Crude oil tank ballasts	3-72
Petroleum reforming	16-3200
Can production forming	200,000

Adapted from Patterson [6].

1.4. Statistics of Oil / Water Pollution

According to a rough estimate about 375 million gallons of oil is released into oceans every year. About 50 % of this oil is because of natural seeping of oil from under ocean oil reserves. Runoff from land sources is the second main cause of oil pollution in oceans which is 35% of total oil released into oceans annually. Transportation of oil through pipes and oil carrying tankers is the third biggest source of oil pollution in oceans that is 12% of total oil released into oceans annually and only 3% of total oil released into oceans annually is because of problems in off-shore drilling of oil [7]. These oil spills results in the disturbance of whole marine ecosystems by limiting the access to oxygen and results in killing hundreds of thousands of organisms living in that environment.

Since the incident of Torrey Canyon of 1967 which discharged 38 million gallons of oil, there have been more than 25 major oil spill incidents in world's oceans. The latest disaster in the Gulf of Mexico was caused by the Deepwater Horizon drilling rig eruption in April 20, 2010, which triggered a sea floor oilfield to release over 60,000 barrels of oil per day (9.5×10^6 L $d^{-1)}$. Gasoline, crude oil and other lubricating oils which consist of Hydrocarbons also include various chemicals which also make their way into the coastal zone from wastewater pollution. Waste oil from cars is most often released into municipal water specifically in underdeveloped countries. This along with the oil washed out from parking area and roads by rain, most of the times reaches the coast. According to an estimate as much as $2.67x10^9$ L of oil reaches to coastal area this way. Until the recent times, the major reason of oil pollution in the oceans was because of run off from land sources. The scenario has now changed and in 1993, half of the oil pollution in oceans was from oil spills and the rest of the half was contributed by land sources. Whereas, it is reported that in 2002 almost 37% of oil pollution in oceans was from land sources whereas the rest of 63% was from oil spills whether accidental or intentional. Table 1.3 shows ten major oil spill accidents from tanker sources, whereas table 1.4 shows four major oil spill accidents from non-tanker sources [4].

Table 1. 3 Top ten major oil spills from oil tankers since Torrey canyon 1967

Position	Ship Name	Year	Location	Spill Size (tons)
1	ATLANTIC EMPRESS	1979	Off Tobago, West Indies	287,000
2	ABT SUMMER	1991	700 nautical miles off Angola	260,000
3	CASTILLO DE BELLVER	1983	Off Saldanha Bay, South Africa	252,000
4	AMOCO CADIZ	1978	Off Brittany, France	223,000
5	HAVEN	1991	Genoa, Italy	144,000
6	ODYSSEY	1988	700 miles off Nova Scotia, CA	132,000
7	TORREY CANYON	1967	Scilly Isles, UK	119,000
8	SEA STAR	1972	Gulf of Oman	115,000
9	IRENES SERENADE	1980	Navarino Bay, Greece	100,000
10	URQUIOLA	1976	La Caruna, Spain	100,000

Source: From the International Tanker Operators Federation LTD. (ITOPF) web site (http://www.itopf.org/knowledge-resources/data-statistics/). With permission of the International Tanker Owners Pollution Federation Limited (ITOPF).

It is estimated that almost 375 million gallons of oil is spilled out into the ocean every yuear which is enough to fill three quarters of entire empire state building. It only makes just 1% of whole water volume in the world's oceans. The matter of concern is not the volume of oil spill but where it ends up. For instance, the famous 'Exxon Valdez' tanker spill has the volume of about 11 million gallons which is less than 10% the size of the 'Ixtoc I' spill. However, the total expenditure for the cleaning and residual damages has been approximated to be 100 times more than that for 'Ixtoc I' spill [7].

Table 1. 4 Top four major non-tanker oil spills

Incident Name	Year	Location	Spill Size (tons)	References
Kuwait/Gulf War	1991	Kuwait/ Persian Gulf	1,600,000	[8]
BP Deepwater Horizon Macondo Well	2010	US Waters Gulf of Mexico 60 miles off the State of Louisiana.	700,000[a]	[9]
IXTOC I Well	1979	Mexican Waters, Bay of Campeche, Gulf of Mexico	Est. 450,000 to 1,400,000	[10]
Nowruz Well during the Iraq-Iran war	1983	Northern Persian Gulf	140,000	[10]

[a] The official estimate of the amount of oil spilled is 4.9 million barrels +/- 10%,8 or a mean of 700,000 tons. (Note that the conversion is barrels x 42 gallons/barrel x 0.0034 tons/gallon = tons8, which is the unit metric tons). Est. is an abbreviation used for Estimate**.**

The largest source of oil pollution in water which is the natural seepage seems to have less harmful effects. The organisms that exist in the area of natural oil seepage have adopted themselves over the period of time and can now not only exist in that environment but can also metabolize the substance released from the seepage. Similarly, the oil spills because of activities of humans also have varying effects. For example, if the oil spill has occurred in the site where the temperature is low, the oil evaporation will take place slowly. On the other hand, oil spills happening in the warmer waters will evaporate and dissolve at faster rate. Component of oil that is lighter in weight will easily evaporate and those components that are soluble will get dissolved. Oil spills that happen in waters far away from the surface, deep down in ocean will go through extensive weathering processes which involve the decomposition of bigger oil droplets into microscopic ones by the wave action [7].

Before the incident of Deepwater Horizon, oil spill accidents were not considered significant because the pollution caused by spilling of oil was not always very noticeable and in the end, the oil was seemed to be decomposed. Consequently, despite of the increased number of oil spill accidents, until the recent times, it was not

considered significant enough for monitoring programs. Many oil tanker spills are not very familiar as they happened far away in deep seas and oceans and so only a small amount of oil reached the coastal areas. In other words these oil were out there safely in the deeper waters where they were engulfed by enormity of seas and oceans. Therefore, only a small number of these spills got under the light of scientific study. These oils spills might have their unnoticed adverse effects on ecosystems of the area of spill. For some of the oil spills in which no severe, long lasting and adverse impacts occurred did not mean that there were no adverse effects at all.

1.5. Major Oil Pollutants

As far as the pollutants are concerned, the composition of waste oil discharged into the oceans and that of crude oil is different. However, one major component of both types of oils is aliphatic or saturated hydrocarbons. The size of these Hydrocarbons lies between one C-1 compound as in Methane to complex molecules with higher molecular size that encompasses hydrocarbon in liquid phase n, waxes as well as solid hydrocarbons. Apart from aliphatic hydrocarbons other type of compounds are also present including aromatics, Asphaltenes and naphtenes etc [11].

Besides that, hydrocarbons from other sources make their way to marine environment. One source is the cuticle waxes from the leaves of superior plants [12-14]. Apart from that, bacteria [15] and phytoplankton [16] also contribute to the hydrocarbons in marine environment. It is important to know whether the hydrocarbon originates from organisms or if it has come from waste discharge of municipalities and run-off. Another important pollutant in petroleum as well as waste and discharged oil is aromatic hydrocarbons in variable quantities. Most significant of these are poly aromatic hydrocarbons. Their presence in water is very crucial as they are toxic compounds. PAH in the water can originate from various sources other than the petrochemical and the origin of PAH is a crucial factor to be considered. On method to figure out the source of PAH is to find out the existence of an alkyl substituted PAH. The degree of substitution is determined by temperature during the process of formation. AT high temperature, unsubstituted PAHs are formed whereas, at low temperature, substituted PAHs are formed in a large number. There is another method to determine the origin of PAH which takes into account ratio between methyl phenanthrenes to phenanthrene PAHs. If the ratio is more than 2 then origin is petro-genic and if the ratio is less than

0.5 the origin is considered to be as pyrogenic. Principal Component analysis can also be carried out to determine the source and origin of PAHs.

1.6. Impact of Oil Pollutants

Many factors that are taken into consideration while determining the effect of oil spill include the nature of oil spilled, the environmental conditions in the area of oil spill, the organisms that are vulnerable to the spill and how far the damage from the site of human activities is.

Various oil spills have only a little effect on human activities or on ecological resources whereas, some oil spills have various impacts both on ecological resources and human health. Different types of fishes, birds, mammals and plants are killed especially those that are in direct contact with the oil spill. The oil spills can also lead to the defective reproductive success of the organisms. Oil pollution can also contaminate the living organisms causing the accumulation of contaminants in organisms in food chain and ultimately affecting the human health. In addition to that, the birds are more vulnerable to the small oil spots, as the oil on their feathers affects their normal insulation process leading to hypothermia. The oil in water behaves as flypaper which traps smaller organisms, ultimately killing them. Larger organisms seeking the trapped food sources will ingest the oil droplets in water, or they may inhale the oil droplets or these oil droplets might stick to their gills as they move through oil emulsion. If the concentration is high they may die as they swim through the emulsion and if the concentration is low they might become impaired. Contamination of fish or their loss can impact the fish market causing in the increased prices of fish. Apart from the direct effect that oil spills have on the organisms, they may also lead to the contamination of beaches and marshes thus, affecting the breeding and feeding grounds of organisms.

Another major effect of oil spillage is found to be on the rocky sea shores as well as on shallow waters where algae were found to be growing in abundance after months and sometimes even after years of spillage incident. The oil caused the accumulation of poison in snails and algae eaters and as a result algae had a chance to grow uncontrollably. The return of snail and other algae grazers at the site of spillage can take more time because of which thick mats of algae forms and it can take a more time to re-establish the disturbed balance As a result of lack of space, due to the abundance of algae other organisms might have difficulty in resettling [17].

Oil spillage can pose damage to small coral building organisms as they are more sensitive to the oil components. Another harmful short-term effect which harbors long term side effects is related to the mangroves. Mangroves grow near the mouths of river where fall into the oceans in soil which is rich in organic materials and is anaerobic. They have root systems that have a special structure called pneumatophores which grow vertically from the horizontal roots and rise above the sediments to keep the root system aerated. If these chimneys like structures become blocked with oil, the mangroves can die. The mangroves hold the muddy soil at a place and if they die the soil won't be able to stay in the place and will be flushed into the oceans and seas [18].

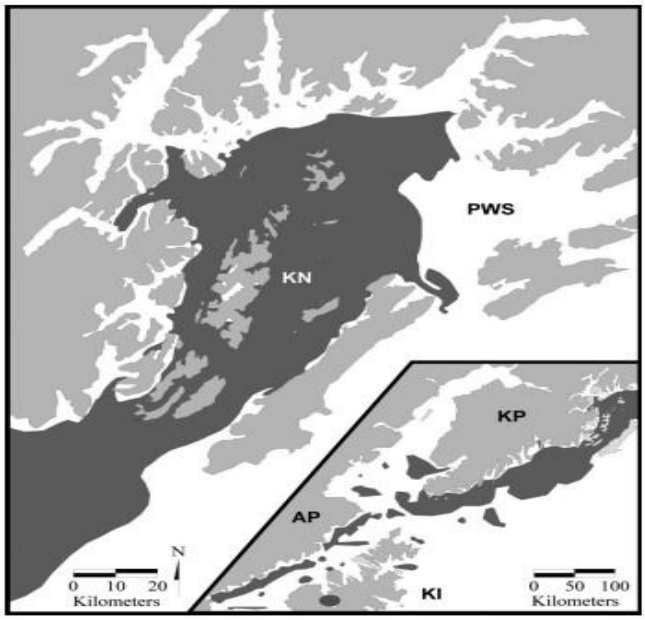

Figure 1. 2 A map of the spread of oil

The shorelines (indicated in black) contaminated to some degree after the grounding of the Exxon Valdez at Bligh Reef in northern Prince William Sound. Oil was transported to the southwest, striking Knight (KN) and other PWS islands, the Kenai Peninsula (KP), the Kodiak Island archipelago (KI), and the Alaska Peninsula (AP).

1.7. Lesson from Nature for Oil / Water Separation

Nature inspired new materials of special wettability are gaining importance now a days that can selectively absorb oil or water from oil-water emulsions. They can be fabricated by taken lesson from nature because there are many biological surfaces that are superhydrophobic in nature from example leaves of Lotus plant. Studies conducted on it showed that its superhydrophobicity is because of its hierarchical roughness (micro-bumps present on its surface) and its surface chemistry which contains a hydrophobic wax. Considering surface roughness and chemical composition as two

important factors two approaches can be used to prepare biomimetic superhydrophobic surfaces [19].

1. Modification of initially hydrophobic materials to make their surface rough
2. Modification of inheritably rough surface by altering the chemical composition or by apply hydrophobic material on it.

The primary parameter to define wetting that is the property of liquid to come in contact with solid surface, is static contact angle. The surfaces exhibiting contact angle less than 90° are called hydrophilic surfaces while surfaces exhibiting contact angle between 90° and 150° are termed as hydrophobic surfaces and the surfaces having contact angle more 150° are called Superhydrophobic surfaces [19]. A more detailed description about relation between contact angle, surface roughness and wettability is shown in figure 1.3.

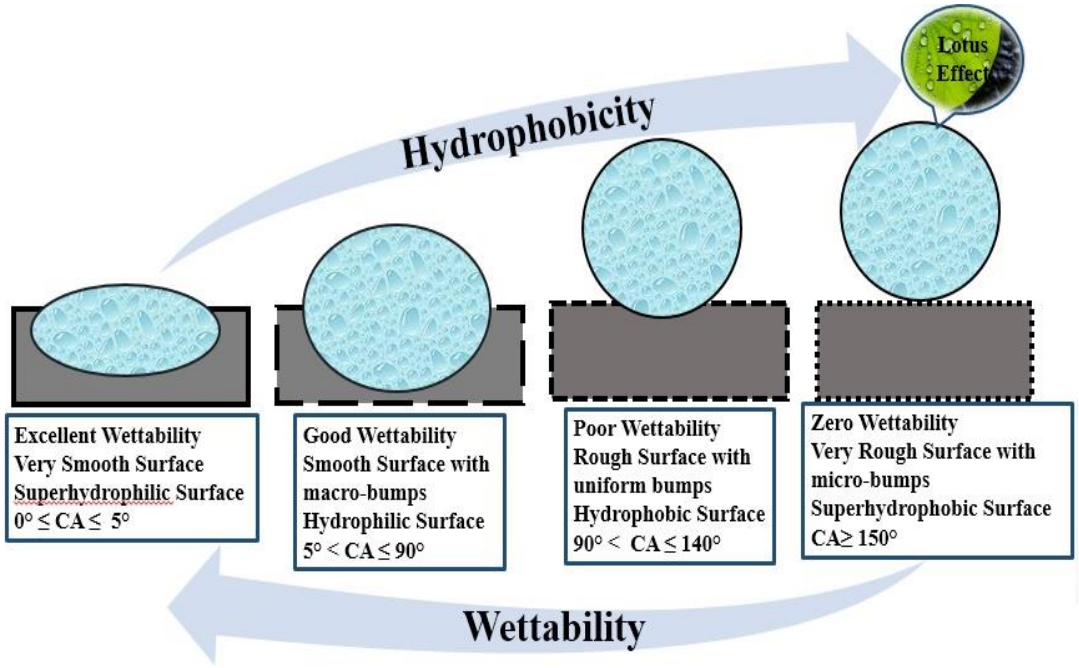

Figure 1. 3 Relationship Between contact angle, wettability and surface roughness

1.8. Metal Organic Frameworks for Oil / Water Separation

Recently efforts have been made in using metal organic frameworks in the oil water separation. Metal – organic frameworks (MOFs), which consist of metal ions and linking ligands which are organic in nature [20], have a consistent and highly adjustable pore structure. With an addition to an excessive variance in secondary building blocks linked with multitopic organic ligands along-with linker topographic anatomy,

chemical functionality and connectivity, they are given priority over traditional porous substances including zeolites and carbon-based materials. Due to these advantages, a MOFs scaffold can be used to give increased adsorption of a specific chemical species, hence providing accurate and speedy separation. Unlike, the conventional inorganic absorbents which have 'rigid' structures, the framework for MOFs because of their organic nature may enable interfaces with the polymers. In addition to that, the increased control over pore structure and functionality at the molecular level is very easy for MOFs as compared to that for zeolites and other inorganic substances [21]. Just like absorbents MOFs can also be used directly as powders [22] and beads [23] or by coating them on a template like sponge [24, 25], mesh [26], membrane and fabric [27]. The variability structure and functionality provides an evidence that MOFs will be more advantageous than other inorganic films and membranes [28].

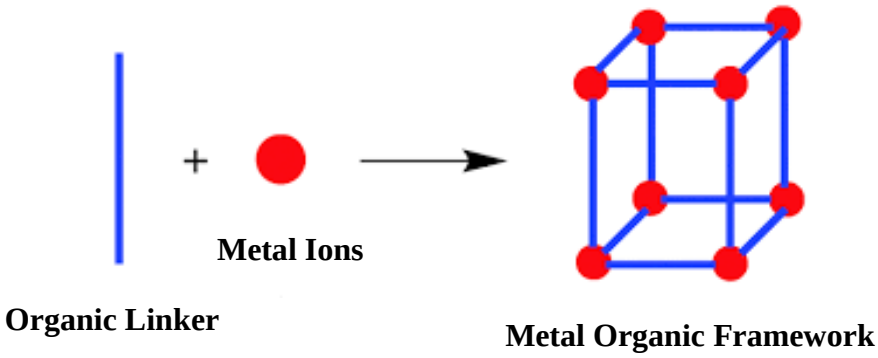

Figure 1. 4 Schematic of Metal Organic Framework

1.9. Long Chain Fatty Acids for Oil / Water Separation

Modification by using low surface energy materials like fluoroalkylsilanes [29], fatty acids[30, 31] and poly polymers [32] is an important process in creating superhydrophobic surfaces. Among these fatty acids because of their inexpensiveness, easy availability and non-wetting properties are gaining increasingly importance in development of tunable functional hydrophobic surfaces [33, 34]. Considering the fact that superhydrophobicity in microstructure is achieved when the length of carbon chain in acid exceeds 16, it can be said that stearic acid which has a C-18 long chain can serve as potential candidate in this regard [35, 36].

1.10. Three Dimensional Porous Materials for Oil / Water Separation

2D porous forms like membranes and meshes of organic / inorganic absorbents and MOFs have gained success in various industrial processes mainly separations but they

get completely fail when a very vast area of water body is effected by oil as in case of oil spill accident in oceans, rivers and lakes. The effected water needs to be collected from vast area, which is very difficult and impractical task, to apply membrane or mesh separation process on it [37]. However 3D porous materials like sponges, foams, aerogels and xerogels do not suffer from this backdraw [38]. The main advantage of using 3D porous materials is that they do not require expensive and specialized equipment for quick and effective removal of pollutants from water. The effectiveness of these 3D porous absorbents is a function of their absorption capacity which is the amount of oil absorbed per unit amount of sorbent used. For this purpose naturally occurring as well as synthetic 3D porous materials are being used but they suffer from backdraw of low separation efficiency because due their ordinary wetting property they absorb water as well in addition to oil [39]. Commonly, two approaches can be used to fabricate 3D porous materials with high hydrophobicity and high separation efficiency.

1. Synthesizing hydrophobic 3D porous materials by using nanoparticles as templates [40, 41].
2. Surface modification of inherited 3D porous materials by functionalization to hydrophobic materials [42].

Three dimensional Sponges of synthetic organic sorbents (polyurethane, polystyrene, polypropylene, nylon, polyester etc.) have regular skeleton with many constructive properties like they are inexpensive, high porous, Low dense, highly elastic, mechanically and chemically stable. Because of these outstanding properties, using approach one, they can be employed for oil/ water separation by incorporating organic, inorganic nanoparticles and their composites in them [43].

1.11. Problem Statement

Though numerous methods for separation of oil/water emulsions and relevant materials have been produced and reported in various studies, almost all of them have inherited drawbacks, and various materials that can fulfill the practical demands are yet in the process of development. Oil water separation technologies utilizing special wettability of 3D porous materials, mimicking the nature i.e. lotus effect, seems to be a promising choice to cope with large scale oil spill accidents compared to 2D porous materials like membranes and meshes but they are generally delicate and can easily get damaged on repetitive use leading to decreased separation efficiency. Consequently, there is a need

for development of economical, recyclable, eco-friendly materials, and simple and efficient technologies for oil/water separation which could separate oil from a large volume of oil/water mixtures effectively.

1.12. Objectives of the Study

Considering separation of oil/water emulsions based on special wettable materials as promising approach, the main objective of this research work is to synthesize a three dimensional sponge with special wettablility by mimicking the lotus effect i.e. optimized surface roughness with micro bumps and optimized surface chemistry with low surface polarity/ energy. The main objective can be defines as follows.

To design a biomimetic highly hydrophobic and highly olephillic fatty acid @ MOF functionalized 3D sponge with excellent oil absorption capacity and reusability.

To achieve the defined objective following set of tasks were performed.

- Fabrication of MOF functionalized sponges with different loadings of MOF.
- Fabrication of fatty acid functionalized sponges with different loadings of fatty acid.
- Fabrication of composite sponges incorporating layers of MOF and fatty acid in different patterns i.e. fatty acid @ MOF @ sponge and MOF @ fatty acid @ sponge.
- X-ray diffractive, Scanning electron microscopic, Fourier transmission infrared spectroscopic, hydrophobic and hydrophilic analysis of prepared 3D sponges.
- Evaluation of oil absorption capacity and recyclability of prepared sponges.

1.13. Scope of the Study

To the best of our knowledge a composite 3D sponge incorporating MOF and long chain fatty acid is not reported yet and in view of the fact that the reported composite sponges of fatty acids exhibit good hydrophobicity but bad absorption capacity as compared to MOF and carbonaceous material based sponges. Herein, utilizing the inherited properties of MOFs i.e. large surface area, controllable pore size and chemical functionality at molecular level, non-wetting / superydrophobic property of fatty acid and regular 3D skeleton of highly porous sponge we fabricated a composite sponge that has optimized morphology and surface chemistry like leaves of lotus plant, and is a

three in one package with hydrophobicity as high as of fatty acid functionalized sponges, high oil absorption capacity as of MOF functionalized sponges and excellent reusability. The composite i.e. stearic acid @ MOF, decorated on sponge template well inherited all properties of its parent components. The coating sequence of MOF and fatty acid i.e fatty acid @ MOF and MOF @ fatty acid was also studied and analyzed. Moreover, a detailed study of the effect of loading of MOF and fatty acid on surface morphology, surface chemistry and thus hydrophobicity is not reported yet. So, it is the current requirement to perform such study and to come up with an optimized loading ratio that gives highest hydrophobicity among all.

1.14. Significance of Study

Keeping in view the limitations of conventional methods and 2D porous materials for separation of oil / water emulsions. The recent study successfully fabricated a three in one package with high hydrophobicity, excellent absorption capacity and reusability for several heavy / light oil / organic solvents. This absorbent material being a three in one package along with its light weigh, easy handling, easy recovery of absorbed oil by simple squeezing/ pressing can be used as a potential candidate where conventional methods and 2D porous materials like membranes as meshes get fail. So this is a significant addition in existing materials for separation of oil water emulsions which can be used for industrial oily effluents as well as oil spill accidents.

Chapter No. 02

Literature Review

2.1. Conventional Oil/water Separation Methods

The four main type of methods used for oil / water separation are

1. Biological method
2. Mechanical method
3. Chemical dispersion method
4. Adsorption method
5. Filtration method

They have many subtypes shown in figure 2.1.

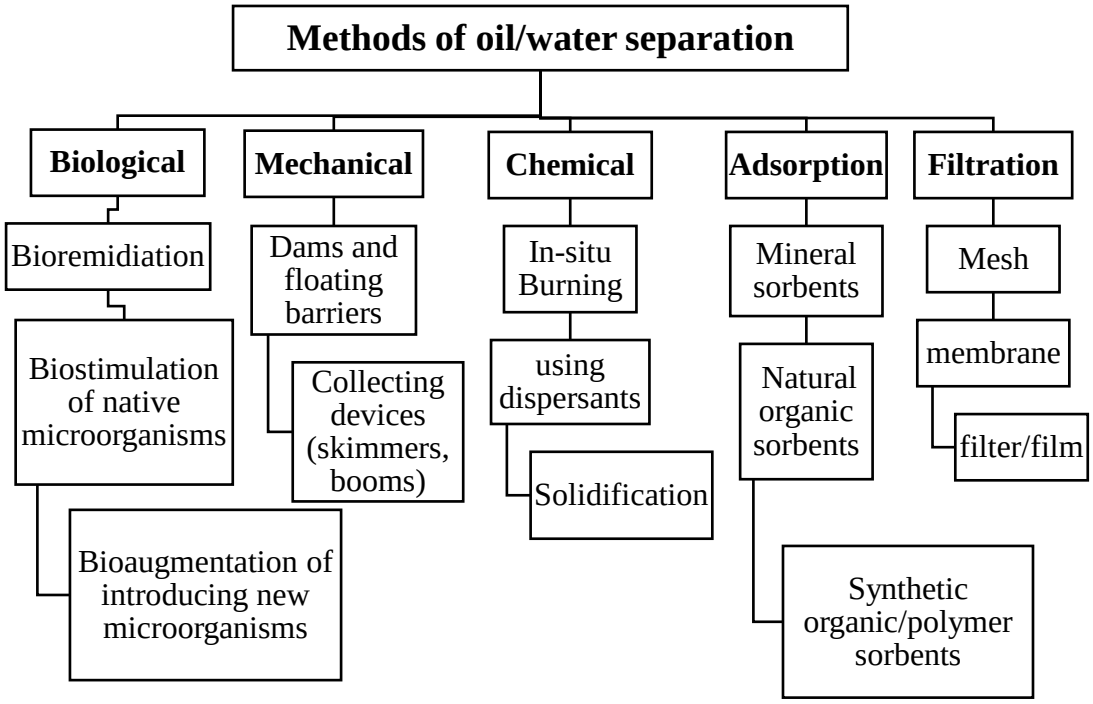

Figure 2. 1 Classification of oil / water separation methods

Biodegradation or biological method is the method whereby oil components are broken-down into simple products like fatty acids and carbon dioxide gas with the help of microorganisms. Biological method also includes strategies which involve the addition of oxygen and nutrients like Phosphorous and Nitrogen into the oil spills to facilitate the bacterial growth [44]. Yet, the major concern regarding biological method is that it

involves using micro-organisms generally bacteria which can decompose the oil. This can result in unbalancing the environment for higher organisms in water. Furthermore, the availability of oxygen is an important factor as the products produced as a result of series of chemical and metabolic reactions in environments lacking oxygen can alter water color, taste, composition and odor making it unfit for organisms to survive in it [45].

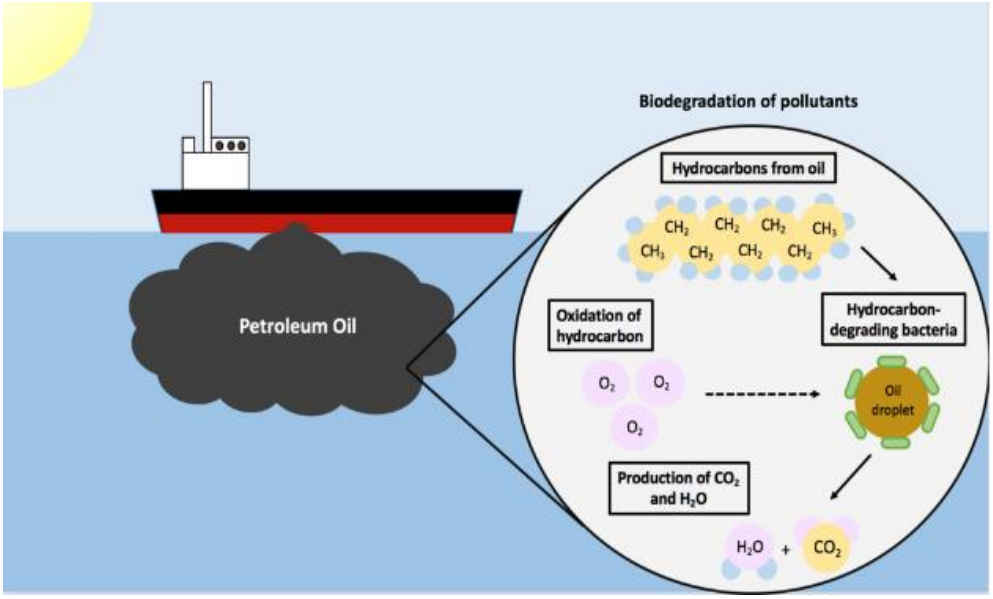

Figure 2. 2 Biological degradation of oil spills using bacteria which decompose hydrocarbons present in oils to produce CO_2 and H_2O

Physical/Mechanical methods mainly include devices that are primary line of defense against disastrous oil spills. They resist the further spread of oil and collect it by mechanical means. These equipment include a diversity of booms and skimmers. Booms are the devices that are stationary and hinder the movement of oil on water preventing it from spreading [46]. The major drawback of using booms is that they require input of a large amount of energy and high pressure in order to work. Skimmers on the other hand can either be movable or stationary that removes floating and or emulsified oil from the surface of water by sucking or scooping the oil into a nearby storage tank. The oil collected by booms and skimmers is then disposed off properly[46]. Some hydrophobic meshes repel water but are able to absorb oil. These hydrophobic meshes can be used along with skimmers to enhance their efficiency [47]**.** Mechanical methods are not applicable during turbulence, high waves and high wind velocity at the place of spill cleanup [48].

Other mechanical methods that are commonly used for oil / water separation of oily waste water from industries are gravity separation and gas flotation. Gravity separation is based on the principal of difference in the density of oil and water. Gas flotation method is based on the density difference but, it takes into account the density difference between bubbles – particle aggregate and water.

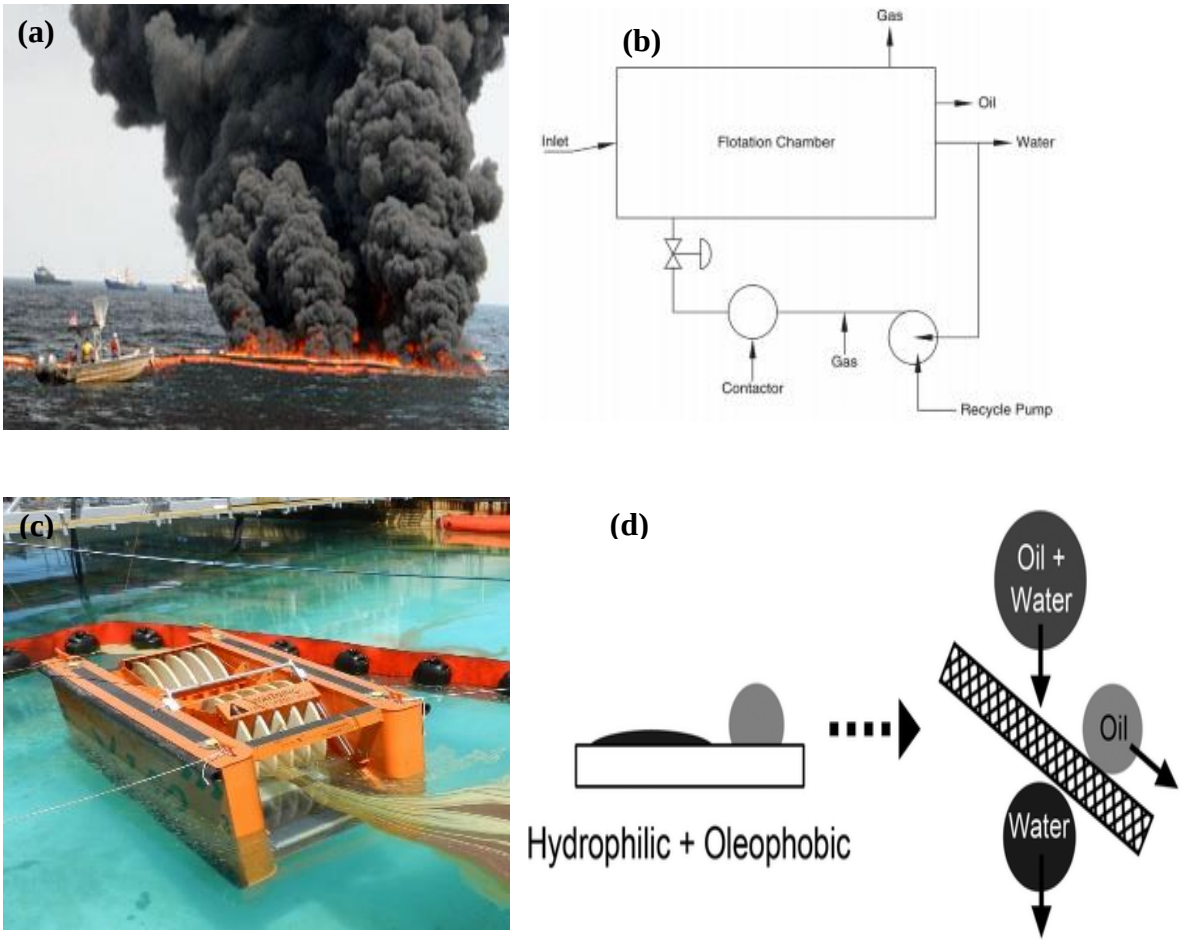

Figure 2. 3 (a) In-situ Burning of spilled oil during Deepwater horizon accident in the Gulf of Mexico, (b) A conventional Gas floatation system for oil/water separation, (c) A conventional skimmer for oil

Most commonly used gas is the Methane gas. It involves many steps. At first gas bubbles are produced then a contact between gas bubbles and water is generated, gas bubbles are then attached with the oil droplets and finally the aggregations of gas bubbles and oil droplets are skimmed and separated [49].

In filtration based separation filtration materials can be prepared by following two approaches [50].

1. Fabrication of porous structures using materials of special wettability
2. Modification by functionalization of already available porous materials.

In filtration based separation, membrane separation serves as an emerging technology in the 21st century. They are usually made of many synthetic materials like polyamide, polypropylene, poly carbonate, cellulose nitrate and cellulose acetate etc. [51]. Oil / water separation filtration materials combines size rejection and wettability together and are made up of or decorated with of super hydrophobic functionalities. This design allows oil droplets to pass through its pores and retains water behind [50]. Membrane separation process can be the best method to use when oil/water mixture to be separated is in in confined space but when it is spread on vast area as in case of oil spill accident in oceans and seas. It is not possible to collect oil from very vast area and apply membrane separation process on it.

Chemical methods on the other hand involve the use of surface active agents (surfactants) which are sprayed on oil water mixture in order to emulsify oil into small droplets [52]. They reduce the interfacial tension between oil and water molecules thus causing dispersion and dilution of oil in water. Because of small size of water droplets and because of their dilution and dispersion in water their rate of evaporation and rate of biodegradation increases [53]. In-situ burning which is burning of oil on the place of spill happening is the method which is the good solution in emergency situation. But it is restricted by conditions of ocean. It devastating for aquatic ecosystem and generate secondary pollutants [54]. Other traditional chemical methods have disadvantages as being money consuming, eco-unfriendly, time consuming and generation of secondary pollutants.

Among all methods sorption is a promising method which can selectively absorb oil or water from oil / water mixture through absorption or adsorption. There are three main types of sorbents used [55].

1. Inorganic mineral sorbents (zeolites, activated carbon, silica, organo-clay, graphite etc.)
2. Natural organic sorbents (leaves, wood waste, wood bark, straw, peat, cellulosic material, moss etc.)
3. Synthetic organic sorbents (polyurethane, polystyrene, polypropylene, nylon, polyester etc.).

These sorbents can be further categorized as shown in figure 2.4.

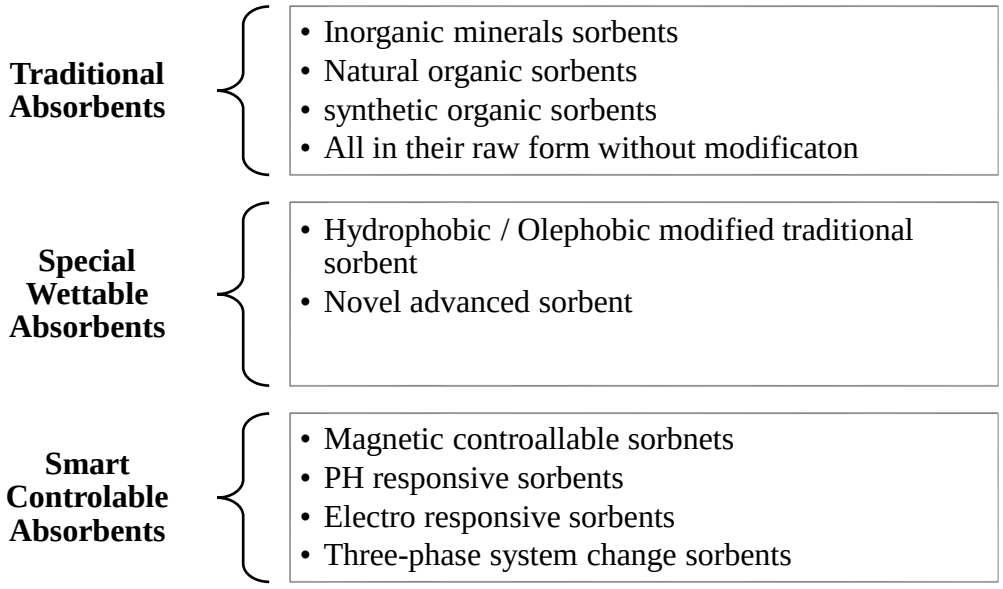

Figure 2. 4 Types of Sorbents

As shown in figure 2.4 they are being used in their raw as well as modified form. Modification through functionalization to convert them to special wettable materials using hydrophobic functionalization agents is gaining importance now a days for selective absorption of oil from oil water mixture. Among these synthetic organic polymers are being extensively used by altering their pore size and surface properties. They can be used as template for coating hydrophobic materials on them and as coating agents on other templates as well. The most useable forms either as templates or coating agents are sponge [56-58], fabric [59], foam [60], mesh [61] and membrane [62]. Their absorbance towards oil is more than 100% of their own weight and even more than this in certain cases.

2.2. Materials

The synthesis of proposed biomimetic hydrophobic 3D sponges was done by using following materials and recent work done is the field of oil water separation using these and other materials is summarized in table 2.1.

2.2.1. 3D Polyurethane Sponge (PU)

Polyurethane is a class of plastic polymers that are made up of organic units joined together with the help of carbamate (urethane) linkages (figure 2.5). They are most commonly manufactured by reaction of di/tri isocynates and polyols [63]. They are available as elastic/rigid material or as porous foam/sponge. Polyurethane foams/sponge can have open cell (flexible), closed cell (rigid) and partially open cell

(semi rigid) morphology. Polyurethane foam/sponge have walls/branches and struts connected together forming voids in-between (figure 2.6). The desired morphology of sponge can be obtained by controlling different parameters e.g. reagents, temperature, pressure, viscosity and presence of organic/inorganic compounds during synthesis and effectively controlling the foaming process [64]. Whatever is the morphology of polyurethane it has same chemical composition i.e. two monomers polymerizing one after the other.

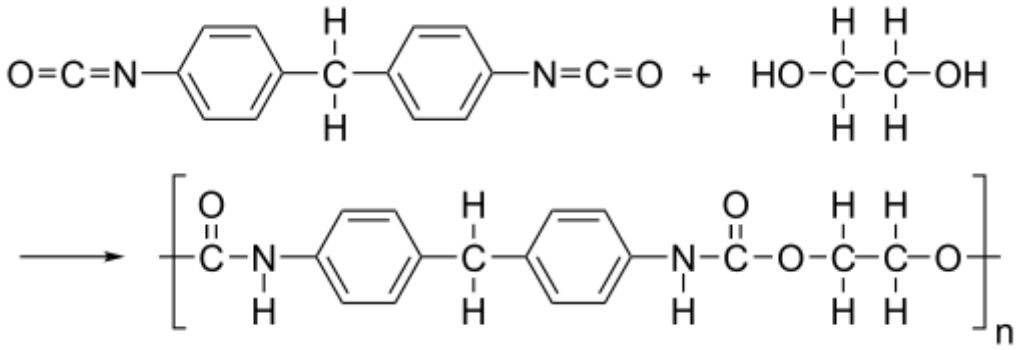

Figure 2. 5 Synthesis and chemical structure of Polyurethane

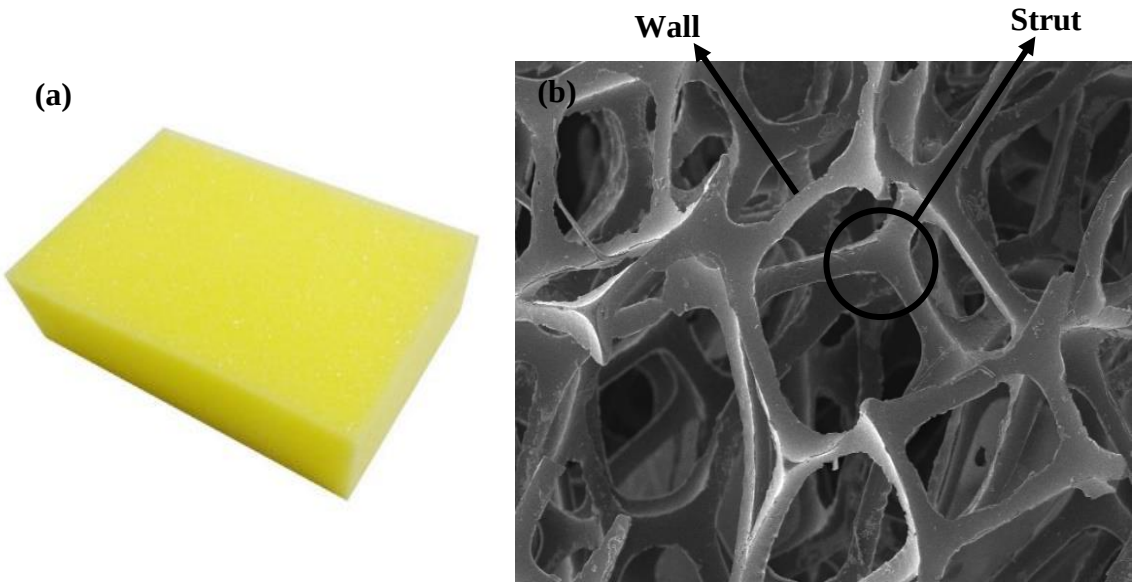

Figure 2. 6 (a) Optical and (b) SEM image of a flexible open cell foam/sponge

2.2.2. Zeolitic Imidazolate Framewok-8 (ZIF-8)

Zeolitic Imidazolate frameworks (ZIFs), a sub class of MOFs are porous hybrids made up of metal ions like Co^{+2} and Zn^{+2} joined together through N atoms of ditopic

imidazole anions to form a three dimensional structure, of four connected tetrahedral units. They can be used in many separation process and catalysis because of their chemical/thermal stability and structural flexibility i.e. tunable pore size and surface functional properties. ZIF-8 that contains Zn^{+2} ions joined through imidazole based linkers is widely explored member of ZIF family (figure 2.7). It consist of six membered pore window that is 3.4 A^o and have a pore diameter of 1.16 nm [65]. The angle between two Zn^{+2} ions linked through imidazole linkers in ZIF-8 is found to be 145^o like in Si – O – Si of zeolites that's why ZIF-8 is structurally similar to SiO_2 frameworks of silicate zeolites [66]. It is one of the best member of MOF family having high crystallinity, flexibility, thermal and chemical stability. It can be used for different purposes like as template to study other materials, as a component of functional composites and as a precursor for the synthesis of different derivatives. Main applications of ZIF-8 are absorption and separation because of its permeability and tunable properties [67].

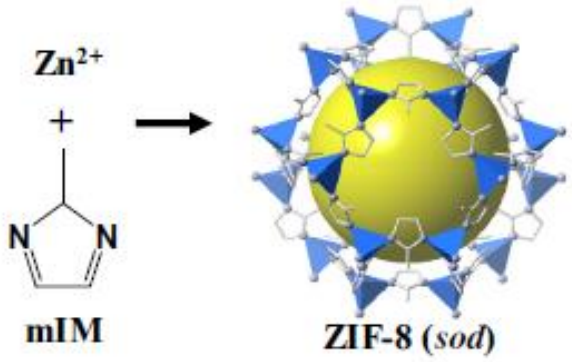

Figure 2. 7 Crystal structure of ZIF-8

2.2.3. Stearic Acid (SA)

Stearic acid is long chain fatty acid with eighteen carbons in its chain. Its other name is octadecanoic acid. In nature it is present in the fats of most plants and animals in the form of mixed triglyceride with other fatty acids and as glycerol ester. It can be synthesized by using animal as well as vegetable fat by hydrolysis and hydrogenation respectively [68]. It has a highly reactive polar carboxyl head that can get attached to metal cations and a non-polar carbon chain that is soluble in organic solvents. It is soluble in ethanol and insoluble in water. Because of its hydrophobic nature it is be

widely used in the field of oil water separation. Figure 2.8 shows the chemical structure of stearic acid.

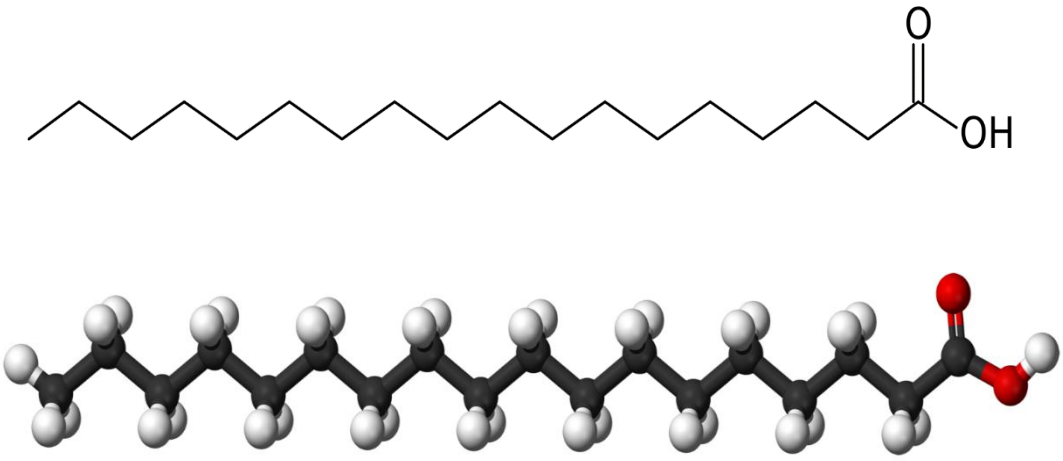

Figure 2. 8 Chemical structure of stearic acid

Table 2. 1 Brief Summary of literature review

Sr. No.	Year	Author	Key Findings	Ref.
1	2018	Ei Ei Sann et al.	In this work ZIF-8 was successfully prepared, contact angle of powdered sample was measured by a previously described method [69] and was used for oil water separation in the form of a tea bag. It has, ✓ WCA =142º ✓ Reusability for twenty cycles ✓ Absorbed oil can be removed by heat and reduced pressure treatment without damaging the particles.	[70]
2	2017	Atanu Jha et al.	In this review materials for oil water separation were summarized based on their separation mechanism i.e. filtration and absorption. Various materials were discussed based on their	[71]

			wettability i.e hydrophobicity or olepillicity. Their inventive aspects and application were also discussed.	
3	2017	Zahra Abbasi et al.	In this work ZIF-8/polymer (PES) composite beads were successfully prepared using one step inversion method for oil/water separation that were, ✓ Easy to handle as compared to ZIF-8 powder. ✓ High absorption capacity as compared to natural absorbent materials. ✓ Low sorption capacity as compared to pure ZIF-8 powder. ✓ Surface area and hydrophobicity increased with increase in ZIF-8 loading. ✓ Retain up to 88 percent of the oil sorption capacity after five regeneration cycles. ✓ WCA=115°	[23]
4	2017	Yahui Cai et al.	A membrane of special wettability was prepared by incorporating ZIF-8 on nanofibers of polyacrylonitrile i.e. PAN@ZIF-8 that showed, ✓ Superoleophobicity under water and superhydrophobicity under oil. ✓ OCA= 159° , WCA= 155° ✓ 99.9% separation efficiency after 20 cycles.	[72]

5	2016	Zixi Kanga et al.	In this work a MOF mesh was first fabricated by in-situ growth of JUC-150 on nickel mesh and was then modified by using PDMS at 220°C (JUC-150@PDMS mesh) to switch its wettability from hydrophobicity or hydrophilicity. It has, ✓ WCA= 143.6° ✓ Separation efficiency=99% ✓ Can be used for upto 5 cycles	[26]
6	2016	Xiaojia Gao et al.	In this work a superhydrophobic/ superolephilic MoS_2 nanosheet sponge was fabricated by exfoliating MoS_2 powder in ethanol solution using ultrasonication and immersing a 3D melamine formaldehyde sponge in it. They also studied the effect of MoS_2 loading on sponge by repetitive dipping and drying. The highest hydrophobicity was given at an optimum loading of 8.4%. They further found out that increase in loading beyond a point creates unsaturated coating that can possibly block sponge pores. Anyhow the prepared sponge can absorb different oil/organic solvents from 82 to 159 times of its own weight while possessing all inherited characteristics of pristine sponge. Because of flexibility of MoS_2 nano sheets and van walls forces between it and 3D sponge it didn't detach from the sponge after manual squeezing. It has, ✓ WCA =150 ± 2 ° at higher loadings ✓ Good absorption and recyclability even at high temperature ✓ Mechanically robust, flexible	[73]

7	2015	Tantan Liu et al.	In this work a graphene oxide coated melamine sponge was prepared by first synthesizing GO by using modified Hummer's method and then coating graphene on melamine sponge by solution template method to get GO/melamine. Then this GO/melamine was reduced to get rGO coated melamine sponge. It showed ✓ WCA= 160 ✓ Reclaim ratio =98% ✓ Absorption capacity of rGO coated sponge increases with loading but decreases on super loading.	[74]
8	2015	Kolleboyina Jayaramulu et al.	In this work a superhydrophobic / superolephilic HFGO@ZIF-8 composite was prepared by adding nano sheets of HFGO during synthesis of ZIF-8. ZIF-8 nano crystals were intercalated between layers of HFGO. It showed ✓ WCA=162°, OCA=0° ✓ Sponge of this material was also prepared that by dipping it in solution during synthesis of ZIF-8. ✓ It showed less absorption capacity ranging fronm150 to 600 wt%.	[75]
9	2012	Duc Dung Ngugen et al.	In this study a superhydrophobic / superolephillic graphene coated melamine sponge was prepared with different loadings of GO by repetitive dipping and drying method. It showed, ✓ WCA=160° at loading 7.3 %	[76]

			✓ Decrease in WCA when loading is increased by 7.3 %. ✓ Absorption capacity upto 165 times of its weight at high loading of graphene for chloroform.	
10	2013	Yue Liu et al.	In this study a reduced graphene oxide coated polyurethane sponge (rGPU) was fabricated by first immersing it in graphene oxide suspension and then reducing it using Hydrazine. They also compared the absorption capacity of rGPU with graphene oxide coated polyurethane sponge (GPU). ✓ rGPU showed a WCA of 127°. ✓ It was found that the absorption capacity of rGPU is higher than GPU for every oil used. ✓ rGPU did not show a significant decrease in absorption capacity even after 50 cycles while in case of GPU it is stable only till 5 cycles because of leaching of GO from GPU	[77]
11	2014	BO Ge et al.	In this work a polyurethane sponge is used as template for coating CNTs-SiO_2 composite that showed superhydrophobic / superolephilic properties. It has ✓ WCA= 158 ✓ Less absorption capacity ranging from 13 to 52 times of it weight for different oils. ✓ Superhydrophobicity after several compression cycles.	[78]

			✓ Constant AC up to five cycles for chloroform and ethanol but it decreases for Rap oil and hexadecane after every cycle.	
12	2019	Zhouqing Xu et al.	This work is related to the fabrication of a hydrophobic composite incorporating a MOF (HPU-13). Cleaned melamine was first modified by immersing it in solution of carboxymethylcellulose sodium (CMC) to make its surface rich of hydroxyl and carboxyl groups and then HPU-13 was coated on it by immersing it in solution of HPU-13. It has, ✓ WCA= 127.1° ✓ High absorption capacity of reaching upto13000 % for trichloromethane.	[79]
13	2018	Zhiwen Lei et al.	This work is related to the fabrication of a ZIF-8 based melamine formaldehyde sponge (MF-ZIF-8 sponge) by using a two step procedure. Firstly, melamine sponge was coated by poly dopamine and then with ZIF-8 by using solvothermal method. The purpose of poly dopamine was to ensure good linkage of ZIF-8 particles with sponge skeleton. It has, ✓ WCA = 140 ✓ Bad absorption capacity reaching to only 3800% for chloroform as compared to other reported sponges. ✓ Absorption capacity only stable till 4 absorption desorption cycles.	[80]
14	2019	Yana Zhang et al.	In this work a highly hydrophobic ZIF-67 coated melamine sponge was successfully prepared by single step in-situ synthesis of ZIF-67 without using any bonding agent. It has,	[81]

			✓ WCA= 142º ✓ Excellent absorption capacity ranging from 77 wt/wt for hexane to 177 wt/wt for chloroform. ✓ The absorption capacity haven't showed a significant decrease even after 20 repetitive uses	
15	2017	He Zhu et al.	In this work a ZIF-8 functionalized hydrophobic sponge was fabricated by using melamine sponge as 3D template by a simple dip coating method (ZIF-8/melamine sponge). A continuous layer of ZIF-8 was formed on the surface of sponge by this methods. It has, ✓ WCA = 120° ✓ Good absorption capacity ranging from 74 to 145 times of its weight for different oils. ✓ Constant absorption capacity for 30 cycles.	[24]
16	2018	Xuemei Zhang et al.	In this work a superhydrophobic magnetic polyurethane sponge was prepared by first coating magnetic Fe_3O_4 nanoparticles and then stearic acid in different concentration on PU sponge. They found out that concentration of stearic acid have great influence on the hydrophobicity because of different surface morphology at different concentrations. The optimum concentration is 2 wt% that has a certain roughness and at high concentrations the surface is rough and uneven causing decrease in hydrophobicity. It has, ✓ WCA = 158 at 2 wt% concentration	[82]

			✓ Stable absorption capacity till five repetitive uses for n-hexane. ✓ Absorption capacity by using different type of oil organic solvents was not reported here.	
17	2017	Viet-Ha Thi Tran et al.	In this work a multistep and multicomponent superhydrophobic sponge was prepared by using polyurethane sponge as template to grow layers of ZnO, Fe_3O_4 and stearic acid on it respectively. The prepared sponge exhibited perquisites of lotus effect i.e. high surface roughness and low surface energy along with magnetic responsiveness. It has, ✓ WCA=161° ✓ Separation Efficiency of > 99%. ✓ Average absorption capacity as compared to other reported sponges ranging from 32.1 to 108.9 g/g for different oils. ✓ Stable absorption capacity over 100 cycles for hexane.	[83]
18	2019	Love Dashairya et al.	In this work a superhydrophobic composite sponge incorporating stearic acid in it was successfully fabricated by Love Dashairya et al by growing polypyrole (ppy) and stearic acid layers on it respectively. It was found that incorporation of stearic acid in this composite increases surface roughness and hydrophobicity as compared to ppy and Stearic acid modified sponges. It has, WCA= ~170° , OCA = 0º	[84]

			Low absorption capacity as compared to other reported sponges for different oils ranging from 70 to 90 times.	
19	2020	Peng Jiang	In this work a cheap and facile method was used to synthesize a hydrophobic sponge incorporating expanded graphite, stearic acid and Fe_3O_4 nanoparticles on polyurethane sponge. Stearic acid created surface roughness in composite sponge, Fe_3O_4 nanoparticles created magnetic responsiveness and graphite caused an increased in its absorption capacity. It has, ✓ Less absorption capacity ranging from 32 to 40 times of its own weight for different oils. ✓ Can be reused for upto 6 consecutive cycles.	[85]
20	2020	Mingbo Shi etal.	This work is related to the fabrication of a superhydrophobic Zr-MOF by reaction amino groups and acid choloride of octadecanoyl chloride. Long alkyl chains reduced surface energy that created superhydrophobicity and increased stability under harsh conditions. Sponge of this material was also prepared by immersing melamine sponge in the suspension of Zr-MOF in PDMS. It has, ✓ WCA=151.7° ✓ Separation efficiency = 99.9% ✓ Absorption capacity ranging from 32.3 to 66.1 g/g. ✓ Absorption capacity reaching upto 80.5% of initial value after 10 cycles for dichloromethane.	[86]

Chapter No. 03

Materials and Methods

3.1. Materials and Chemicals

PU sponge and vegetable oil were purchased from local market. Petrol and diesel were purchased from local fuel station. Deionized water was purchased from Vitro Diagnostic Laboratories Islamabad. Methanol, Ethanol, 2-methylimidazole, Stearic acid and Chloroform were purchased from Sigma-Aldrich. Zinc nitrate hexahydrate ($ZnNO_3.6H_2O$) was purchased from UNI-CHEM chemical reagents. N-hexane was purchased from Daejung Reagents Chemicals and methyl orange was purchased from EYER China.

3.2. Cleaning of Sponge

The PU sponge was first cut into small cubes of 2×2×2 cm. Then pieces of sponge were ultrasonically cleaned for 30 min in ethanol followed by drying in oven at 40 °C. The cleaned sponges were immediately weighed (m_{raw}) and used for further treatment after taking out of the oven to avoid any moisture absorption.

3.3. Synthesis of MOF Functionalized Sponge (ZIF-8 @ Sponge)

As shown in figure 3.1 firstly, 0.735g zinc nitrate hexahydrate was added in 25 mL of methanol and magnetically stirred for 5 min. A piece of cleaned sponge was added to this solution and again stirred for 2-3 min. Then a clear solution of 2-methlyl imidazole (Hmim) in 25 mL methanol was slowly added to the 1st solution under vigorous stirring and allowed to stir at this speed until it turns milky. After the solution has turned milky the speed was slowed down and it was allowed to stir at this speed for 24 hours. Then sponge was carefully taken out of the solution with the help of tweezer without compressing it, washed three times with De-ionized water and dried in oven at 60°C for 6 hours. After taking out of the oven it was immediately weighed again (m_{coated}) to avoid moisture absorption. The remaining solution was centrifuged and washed with ethanol at 400 rpm to get ZIF-8 powder. Five such samples with different Zn^{+2} : Hmim : MeOH shown table 3.1 were prepared for the sake of comparison. Loading ratio % was calculated by using eq. 3.1.

$$Loading\ Ratio\ \% = \frac{m_{coated} - m_{raw}}{m_{raw}} \times 100 \qquad \text{Eq (3.1)}$$

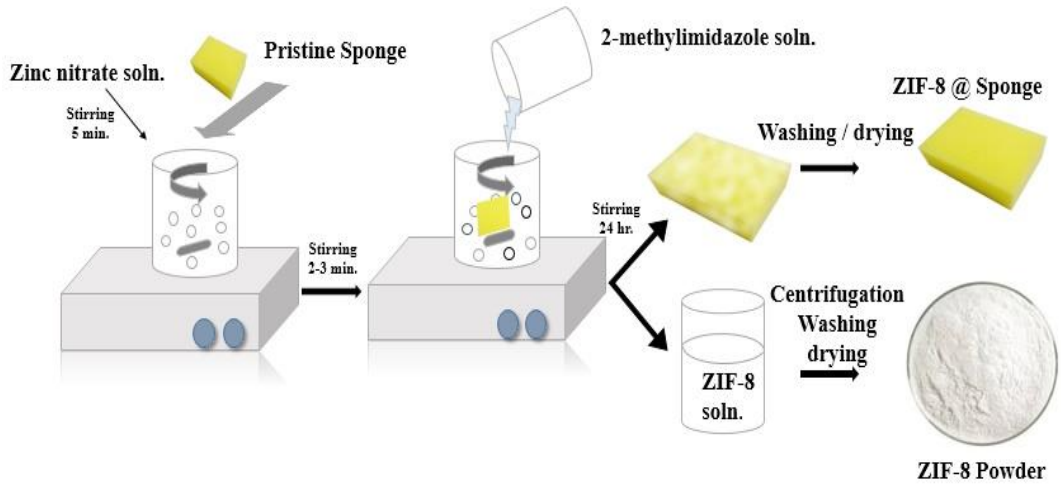

Figure 3. 1 Schematic diagram for synthesis of ZIF-8 @ Sponge

3.4. Synthesis of Stearic Acid Functionalized Sponge (SA @ Sponge)

As shown in figure 3.2 firstly stearic acid was dissolved in ethanol and stirred for 30 min to form a homogeneous suspension. A piece of washed sponge was added to this suspension and again stirred for 6 hours to allow the attachment of long chains of stearic acid on the surface of sponge. The sponge was then carefully taken out of the suspension without squeezing and dried in oven at

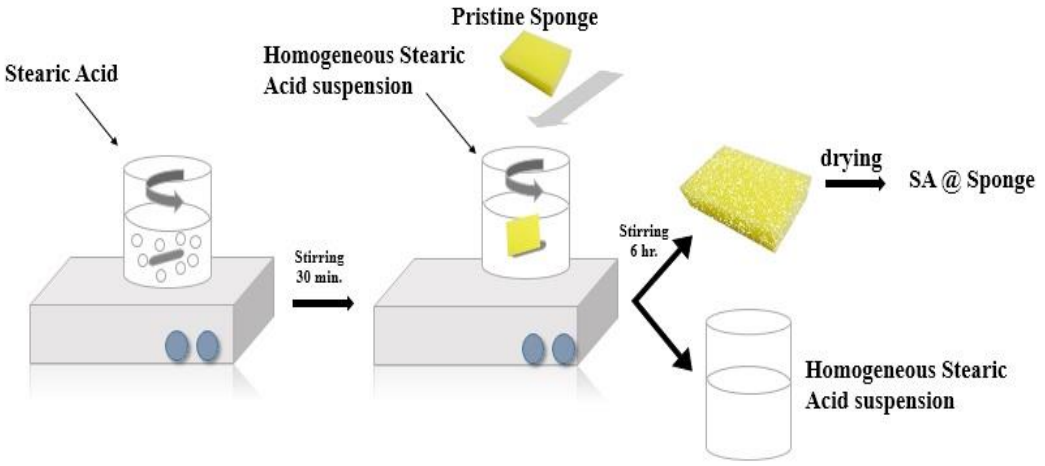

Figure 3. 2 Schematic diagram for synthesis of SA @ Sponge

40º C for 6 hours. Four such samples as shown in table 3.2 with different wt% of stearic acid were prepared for the sake of comparison.

3.5. Synthesis of Composite Functionalized Sponge (Composite @ Sponge)

3.5.1. Synthesis of SA @ ZIF-8 @ Sponge

Depending upon the results of contact angles of ZIF-8 @ sponge samples, composite sponges with fixed amount of ZIF-8 and variable amount of stearic acid were prepared by the following method. The ZIF-8 sponge was first prepared by the method as described in section 3.3 to grow a layer of ZIF-8 on pristine sponge. Then a layer of stearic acid was grown on the ZIF-8 @ sponge by the method as described in section 3.4 to form SA @ ZIF-8 @ sponge, followed by drying in oven at 40 ºC for 6 hours. Four such samples as shown in table 3.3 with different wt% of stearic acid were prepared for the sake of comparison.

3.5.2. Synthesis of ZIF-8 @ SA @ Sponge

The SA sponge was first prepared by the method described in section 3.4 to grow a layer of stearic acid on pristine sponge. Then a layer of ZIF-8 was grown on SA @ sponge by the method as described in section 3.3 to form ZIF-8 @ SA @ sponge, followed by drying in oven at 40 ºC for 6 hours.

3.5.3. Synthesis of SA @ SA @ ZIF-8 @ Sponge

SA @ ZIF-8 sponge was first prepared by the method described in section 3.5.1 to grow a layer of ZIF-8 and stearic acid on sponge respectively. Then another layer of stearic acid was coated on SA @ ZIF-8 @ sponge by the method as described in section 3.4 to form SA @ SA @ZIF-8 @ Sponge.

Table 3. 1 Relationship between reactants ratio and loading ratio % of ZIF-8@ Sponge samples

Sample	**Zn^{+2} :Hmim: MeOH (molar ratio)**	**Loading ratio %**
Z1S	1 :8.08: 499.75	1.90
Z2S	1 :8.08: 249.87	3.46
Z3S	1 :8.08: 166.58	5.01
Z4S	1 :8.08: 124.93	6.26
Z5S	1 :8.08: 099.90	7.30

Table 3. 2 Concentrations of stearic acid used to prepare SA @ Sponge samples

Samples	Concentration of Stearic acid (wt%)
S1S	1 wt%
S2S	2 wt %
S3S	3 wt%
S4S	4 wt%

Table 3. 3 Concentration of reactants used to prepare SA @ ZIF-8 @ Sponge samples

Samples	Concentration of Stearic acid (wt%)	Zn^{+2} :Hmim: MeOH (molar ratio)
S1Z4S	1 wt%	1 :8.08: 124.93
S2Z4S	2 wt %	1 :8.08: 124.93
S3Z4S	3 wt%	1 :8.08: 124.93
S4Z4S	4 wt%	1 :8.08: 124.93

Table 3. 4 Concentration of reactants used to prepare ZIF-8 @ SA @ Sponge and SA @ SA @ ZIF-8 @ Sponge samples

Samples	Concentration of Stearic acid (wt%)	Zn^{+2} :Hmim: MeOH (molar ratio)
Z4S1S	1 wt%	1 :8.08: 124.93
S1S1Z4S	1wt% and 1 wt%	1 :8.08: 124.93

3.6. Characterization

Several characterization techniques i-e- X-ray diffraction, Scanning electron microscopy, Fourier transmission infrared spectroscopy and sessile drop technique were performed to study the physiochemical properties of pristine and coated sponges.

3.6.1. X-ray Diffraction Technique

To determine crystalline materials present in pristine and in ZIF-8 coated sponges X-ray Diffraction technique was performed by using a diffractometer, Theta-Theta, STOE, Germany (230 VAC, 50 Hz and 6,5 KVA) provided with Cu Kα radiation.

Sponges coated with stearic acid were not analyzed by this technique as stearic acid is not a crystalline material. The range of 2θ was selected from 0 to 60 degrees. A piece of sample sponge equal to the size of diffractometer's stub was cut and placed on it which was fixed in sample holder. Then Cu kα radiations with wavelength 1.54 Aº were made to fall on the sample and were received by detector while moving in circle around the sample. The diffraction patterns were produced on computer screen and were analyzed later. The Schematic of working principle of X-ay diffraction technique is shown in figure 3.3.

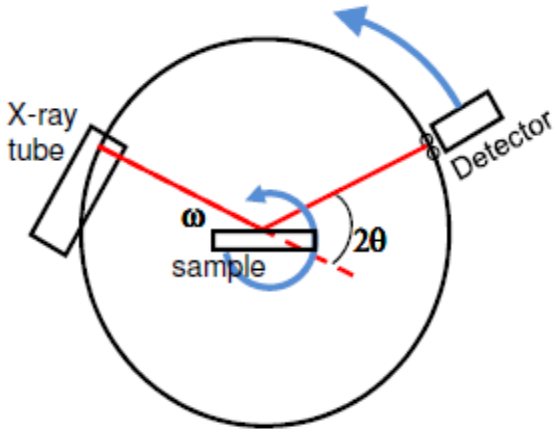

Figure 3. 3 Schematic of working of x-ray diffractometer

3.6.2. Scanning Electron Microscopy

Microscopic morphological and microstructural analysis was done to check the coverage of coating materials on sponge by using a Scanning Electron Microscope, JSM-6490A, JEOL, Japan, at different magnifications. A small piece of sample to be investigated was cut and it was sputtered with Gold at 10 KV. Then the gold coated sample was placed in sample holder and scanned by forcing a beam of electron on it. The incident electrons after interacting with atoms at different depths in sample along with secondary electrons, received by detectors, displayed data on output device in form of images. The main components of SEM are shown in figure 3.4.

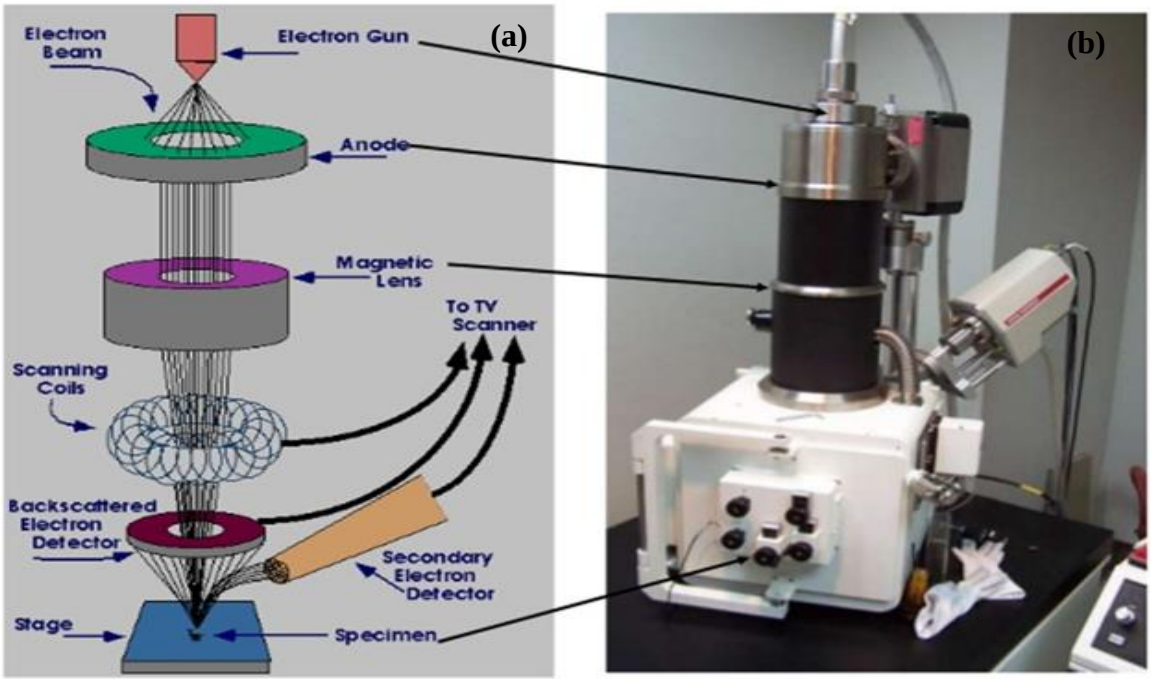

Figure 3. 4 (a) Schematic and (b) Optical image of scanning electron microscope

3.6.3. Fourier transmission infrared spectroscopy

Considering chemical composition and functional groups as an important factor for hydrophobicity and hydrophilicity, pristine and coated sponges with best hydrophobicity from every category were analyzed by using a Fourier Transmission Infrared Spectrometer, Spectrum 100, PerkinElmer, America. Firstly, the sample for FTIR analysis was prepared by using standard method of solid sample preparation. For this the sample sponge to be investigated was cut into tiny and thin pieces to allow infrared radiations to pass through it. Then 200mg of infrared grade KBR and 2mg of pieces of sample were used to make a pallet by squeezing them in a hydraulic press. The pallet was placed in FTIR spectrometer and was made to receive infrared radiations from the source. The spectrometer measured the amount of radiations absorbed at different frequencies and displayed the data in the form of spectrum of wavelength

ranging from 4000 cm^{-1} to 1000 cm^{-1} versus transmittance on computer screen and analyzed. The working principle of FTIR is shown in figure 3.5.

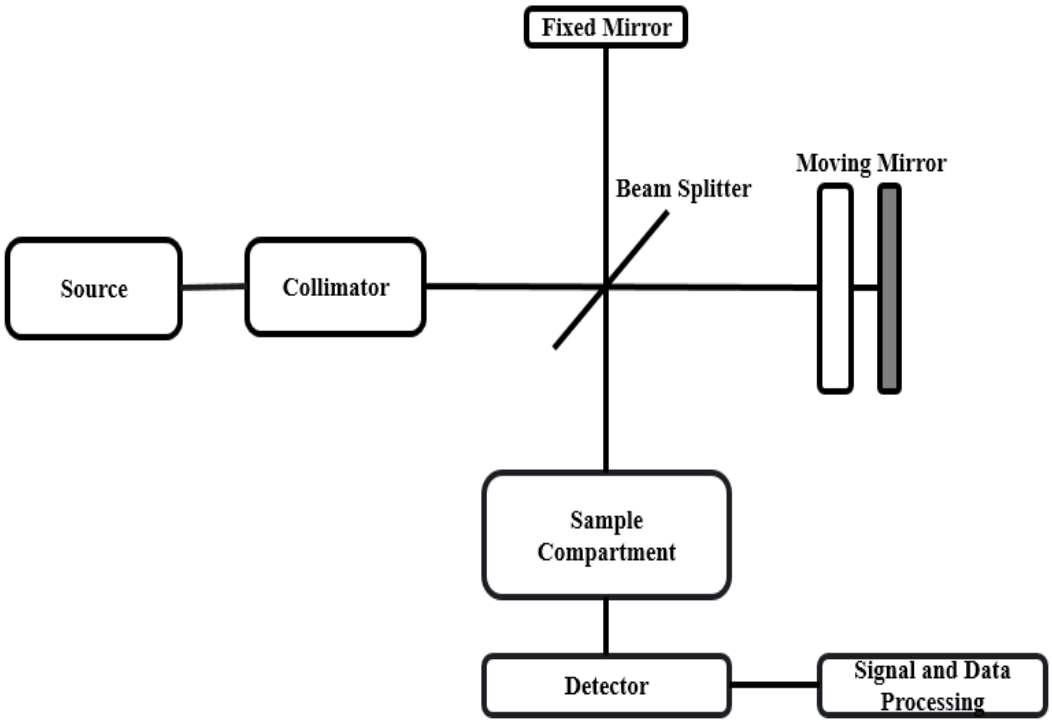

Figure 3. 5 Schematic of fourier transmission infrared spectrometer

3.6.4. Sessile Drop Technique

Sessile drop technique was used to measure water contact angle by using Drop Shape Analyzer, DSA25S, KRUSS, Germany, by dropping water droplet at different locations on the sponge surface. The main components of drop shape analyzer (figure3.6) used for this test are light source, motor driven syringe, moveable sample holding stage, camera and computer. The syringe was first filled with solvent. The sample with flat surface to be investigated was placed on stage just below the syringe and position of stage and syringe was adjusted so as to get clear image on computer screen. Then a drop was made from syringe to make a sessile drop i.e., liquid droplet sitting on the solid surface. The contact angle was measured between so called base line and outer surface of sessile drop by drawing lines with the help of software.

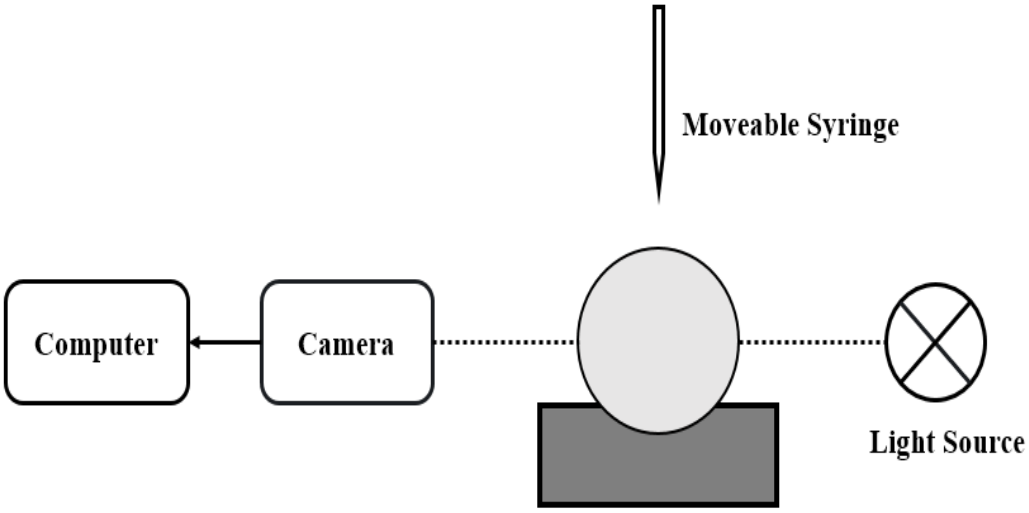

Figure 3. 6 Schematic of drop shape analyzer

3.7. Oil / Organic Solvent Absorption Test

Considering diesel and some organic solvents as main pollutants in oily waste water, absorption capacity (AC) was calculated by oil adsorption short test described in ASTM F716. Five different oils/organic solvents (diesel, petrol, n-hexane, chloroform, vegetable oil) with different densities i.e. less than and greater than water were chosen to perform this test. Briefly oil / organic solvent was mixed in deionized water in volume ratio of 1:10. A piece of coated sponge was first weighed (m_i) and placed in oil water mixture. The sponge was allowed to float on the surface of mixture for 15 min $\mp$ 20 s. It was then taken out with the help of tweezers, giving a dripping time of 30 $\mp$ 3s to drain additional oil and then immediately weighed (m_f) again to avoid drainage of additional drops. Absorption capacity as grams of oil absorbed per grams of sponge was calculated using eq.3.

$$Absorption\ Capacity\ (g/g) = \frac{m_f - m_i}{m_i} \qquad \text{Eq (3.1)}$$

This test was triplicated for all samples and a mean was calculated to give an average absorption capacity, shown in figure 4.22.

3.8. Reusability and Recyclability Test

Considering reusability and recyclability (Rc) as an important factor for the practical application, reusability and recyclability test was performed for one ZIF-8 coated and one composite sample having optimum value of hydrophobicity and absorption

capacity among all. Diesel and chloroform were chosen randomly as test solvents. The procedure adopted was same as oil adsorption short test, except at the end of each cycle the sponge was manually squeezed to recover absorbed oil, weighed and then used again for next cycle. This experiment was done for ten cycles and absorption capacity and collection capacity was calculated for every cycle by using following formulas.

$$AC_x\ (g/g) = \frac{m_{xf} - m_{xi}}{m_{xi}} \qquad \text{Eq (3.2)}$$

$$CC_x\ (g/g) = \frac{m'_{xf} - m_{xi}}{m_{xi}} \qquad \text{Eq (3.3)}$$

Where, x is the cycle number, m_{xi} is the initial mass of sponge at the start of cycle x, m_{xf} is the final mass of sponge at the end of cycle x , m'_{xf} is the mass of sponge after squeezing it at the end of cycle x.

Chapter No. 04

Results and Discussion

Considering successful coating on sponge skeleton, chemical composition, surface roughness and hydrophobicity as important factors to achieve defined objectives, several characterization techniques were performed, critically analyzed and are discussed below.

4.1. X-Ray Diffraction Analysis

X-ray diffraction patterns of pure ZIF-8 and pristine polyurethane sponge (PS) shown in figure 4.1 (a, b) respectively are well consistent with one available in literature [72, 87]. The presence of sharp peaks at around 2θ= 7, 10, 12, 15, 16 and 18 correspond to planes at (110), (200), (211), (220), (310) and (222) respectively, showing highly crystalline nature of ZIF-8 [88]. The pristine sponge shows a significant hump around 2θ = 20 justifying the amorphous nature of polyurethane and a sharp peak at 2θ = 29 is because of PPG crystals in soft segments [89]. The peaks of pristine sponge are still there on all ZIF-8 @ Sponge samples as shown in figure 4.1 (c-g), showing that it is not damaged during coating. The development of characteristic peaks of ZIF-8 on the hump of sponge can be clearly seen in all ZIF-8 @ Sponge samples. This shows that ZIF-8 has been successfully grown on sponge skeleton however, the intensity of these peaks is changing by change in loading ratio %. These results are also consistent with their SEM and FTIR results as well.

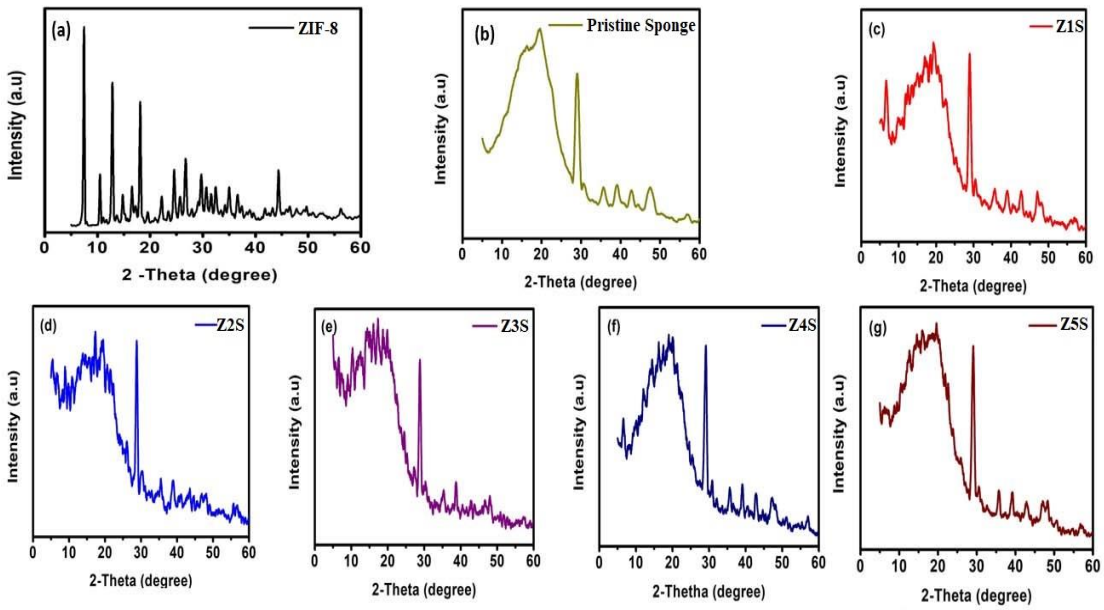

Figure 4. 1 XRD pattern of (a) ZIF-8, (b) pristine sponge, (c) Z1S, (d) Z2S, (e) Z3S, (f) Z4S and (g) Z5S

4.2. Scanning Electron Microscopic Analysis

4.2.1. Scanning Electron Microscopic Analysis of PS and ZIF-8 @ Sponge Samples

Figure 4.2 (a-c) shows the clean and smooth branch's surface of washed pristine polyurethane sponge at different magnifications. No particle can be seen deposited on the surface of pristine sponge. In Z1S, figure 4.3 (a-c), there are some particles of ZIF-8 adhered to surface giving very small loading. The particles have not covered the whole surface but are aggregated on one place and high magnification images conformed that they have not attained the hexagonal shape. This can be attributed to the reason that very small concentration of precursors resulted in very less nucleation and growth of crystals. On further increasing the concentration, particle's morphology changed to hexagonal. In Z2S, figure 4.3 (d-f), same kind of behavior regarding aggregation of particles on one place was observed and some particles were seen dispersed on the surface as well, giving higher loading than Z1S. In Z3S, figure 4.3 (g-i), because of higher concentration of precursors the development of more ZIF-8 particles can be seen on the surface. The ZIF-8 particles have completely covered some areas of sponge, and some areas are still uncovered, making the surface patchy. On areas covered by ZIF-8 particles, cracks can be clearly seen making voids inside the ZIF-8 layer and giving macroscale roughness that is not good for achieving hydrophobicity. As compared to Z2S the loading of Z3S was significantly increased because of higher nucleation and growth of ZIF-8 particles. In Z4S, figure 4.3 (j-l), the loading was further increased that covered entire branches of sponge, making a smooth but not patchy layer of ZIF-8 on the surface. The high magnification images confirmed the presence of microscale roughness that is good for achieving hydrophobicity. On further increase in concentration the loading was also increased. The SEM images, figure 4.3 (m-o), showed that the too much increased concentration of precursors facilitated the rapid nucleation and growth of more ZIF-8 particles, that covered the entire surface but because of this rapid nucleation and growth, the particles got agglomerated giving non uniform distribution of ZIF-8 on the surface creating macroscale roughness and voids on the surface. So, from scanning electron microscopic analysis it can be concluded that in in-situ growth of ZIF-8 on polyurethane sponge the loading increases by increase in precursors concentration but a uniform layer of ZIF-8

on sponge with microscale roughness can only be formed at a specific concentration as is the case with Z4S.

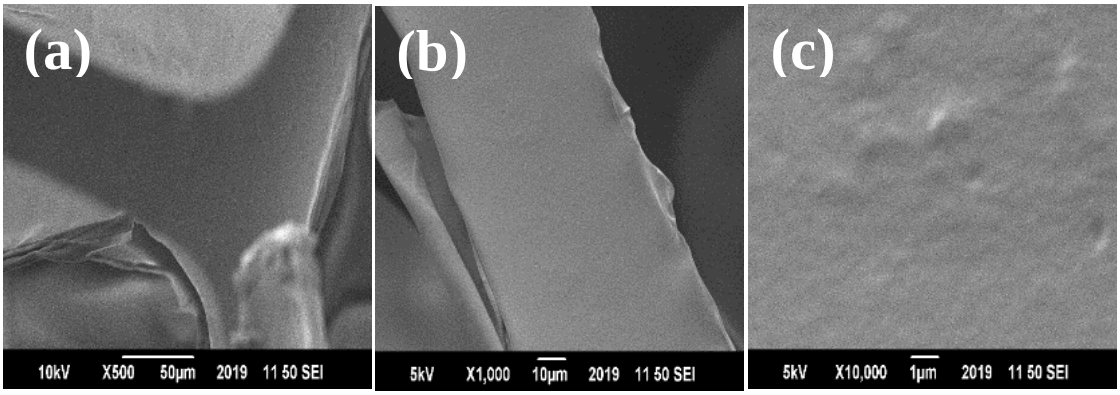

Figure 4. 2 SEM images of pristine sponge at different magnifications

4.2.2. Scanning Electron Microscopic Analysis of SA @ Sponge Samples

Figure 4.4 shows the SEM images of sponges after coating with different concentrations of stearic acid. Wrinkled Layer of stearic acid can be clearly seen on all samples and is consistent in resemblance with available in literature [90], however the morphology of coated layer is changing with change in concentration that might affect the hydrophobicity as well. Figure 4.4 (a-b) and figure 4.4 (c-d) show the SEM images of sponge coated with 1 and 2 wt% of stearic acid respectively. The micro/nanoscale protrusions of stearic acid nano-sheets with folding edges can be clearly seen on sponge's branches endowing it with high surface roughness, however the sponge skeleton is still intact showing that it is not damaged during coating process. Deep analysis shows that in S2S the protrusions seem to be stronger, heightened and not so arranged as compared to S1S because of higher concentration of stearic acid. Figure 4.4 (e-f) shows the SEM images of S3S. Here, also the stearic acid have fully covered the sponge surface but because of high concentration the protrusions are more overlapped and tangled with each other. This situation in S2S and S3S can possibly contribute to macroscale roughness to some extent. Figure 4.4 (g-h) shows the SEM images of S4S, which shows that on further increase in concentration to 4 wt% the overall sponge surface became smooth with some protrusions of facing outside. The possible reason can be the too much concentration because of which the channels between the protrusions got filled with stearic acid itself making it smooth. In other words because of multilayers of stearic acid the protrusions of layers got interlocked making it smooth that will definitely reduce its hydrophobicity. Anyhow, the scanning electron microscopic analysis conformed that stearic acid have been well coated on sponge

surface, without damaging its three dimensional skeleton. The presence of stearic acid was also confirmed by FTIR and analyzed.

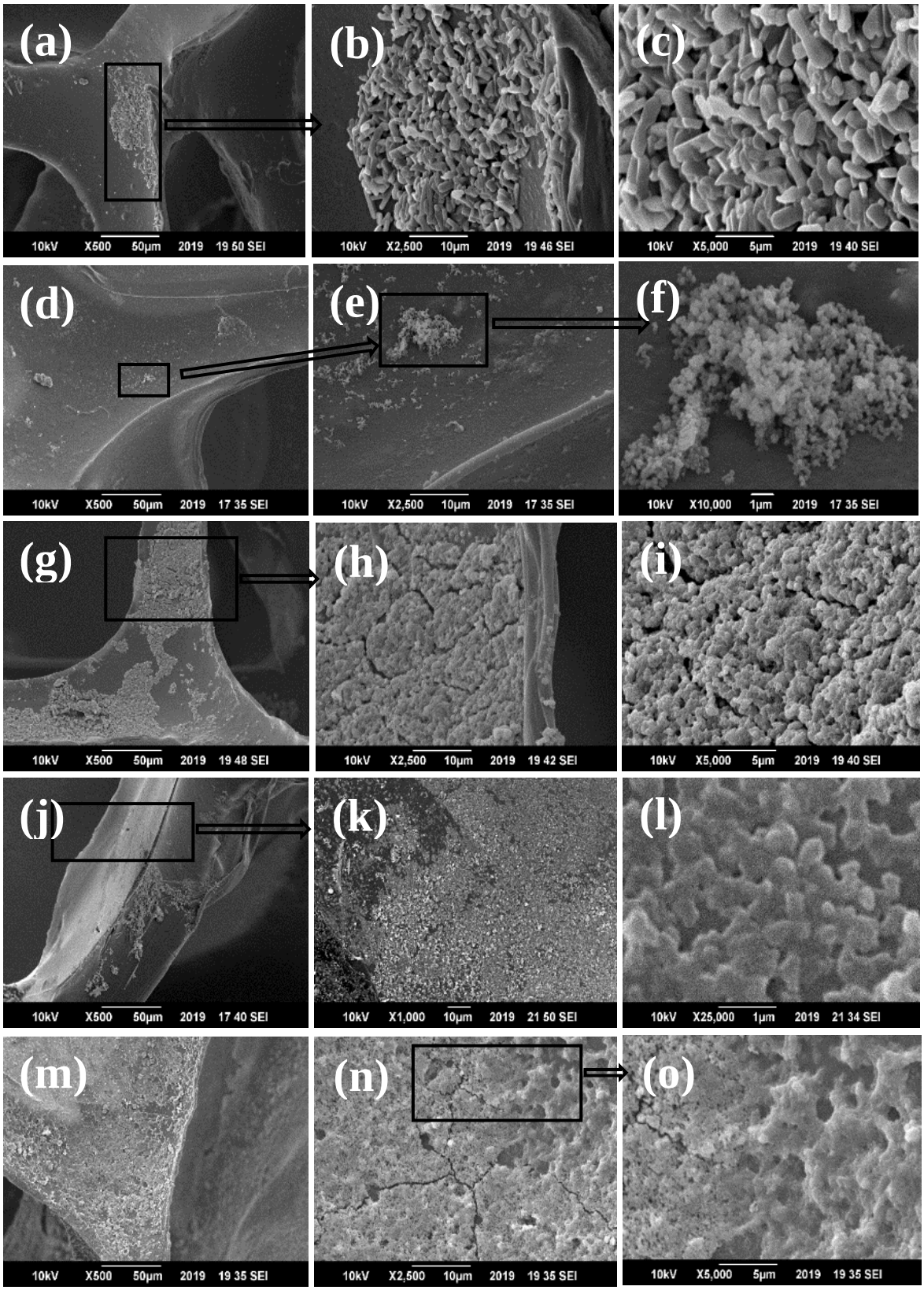

Figure 4. 3 SEM images of (a-c) Z1S, (d-f) Z2S, (g-i) Z3S, (j-l) Z4S, (m-o) Z5S at different magnifications

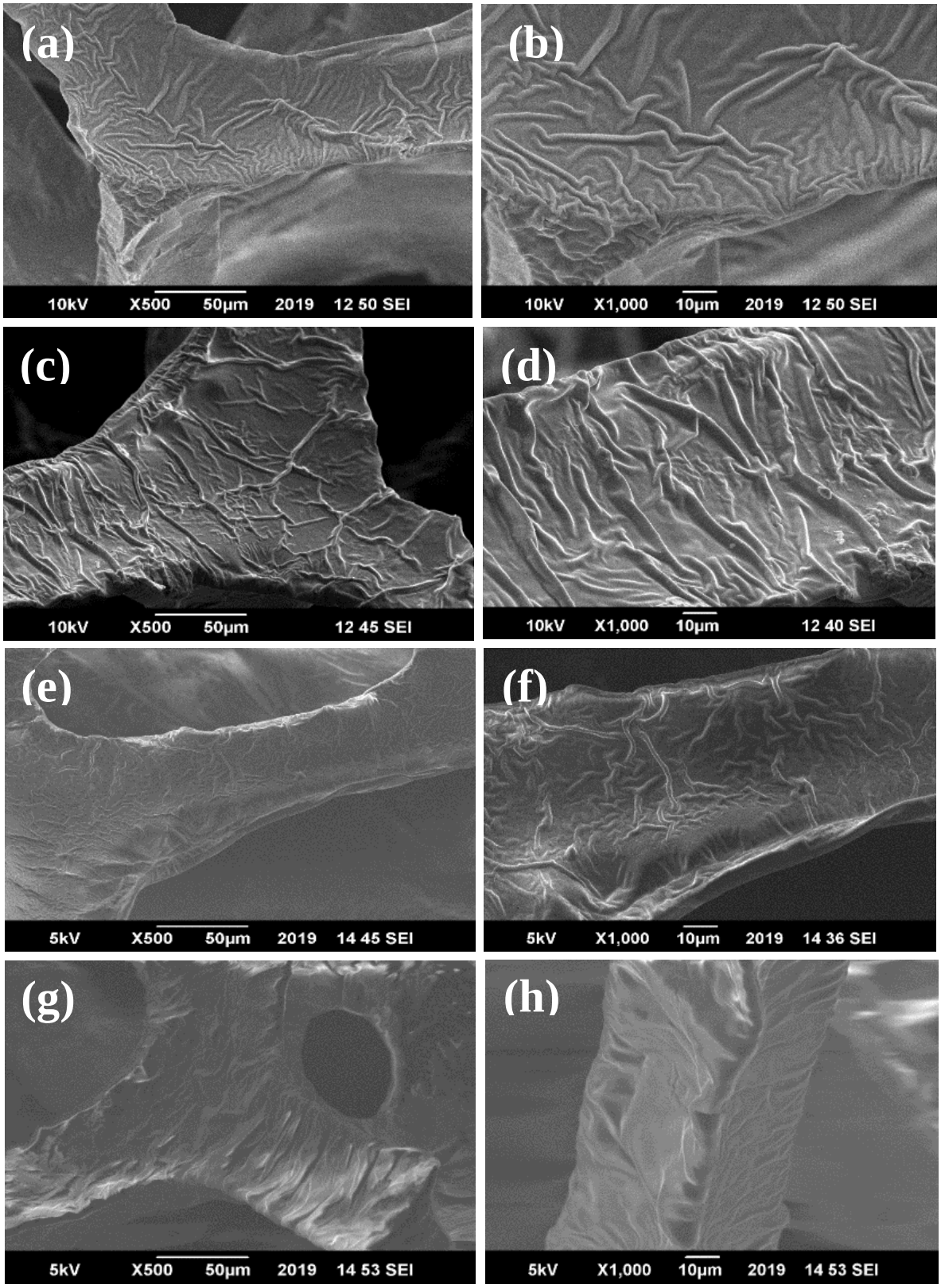

Figure 4. 4 SEM images of (a-b) S1S, (c-d) S2S, (e-f) S3S, (g-h) S4S at different magnifications

4.2.3. Scanning Electron Microscopic Analysis of SA @ ZIF-8 @ Sponge Samples

In SA @ ZIF-8 @ sponge samples same morphological behavior as SA @ sponge samples is observed because stearic acid is the outer layer in composite samples and is in same concentration as stearic @ sponge samples. Figure 4.5 (a-b) shows SEM images of S1Z4S with same wrinkled pattern as S1S. The protrusions of stearic acid can be clearly seen that are providing it with suitable roughness for gaining hydrophobicity. Figure 4.5 (c-d) shows SEM images of S2Z4S whose wrinkled pattern of stearic acid is congruent with S2S. The protrusions of stearic acid seem to be stronger, heightened and not so arranged as compared to S1Z4S which might affect the hydrophobicity. Figure 4.5 (e-f) shows SEM images of S3Z4S. Here the stearic acid is fully coated on sponge surface but because of too much concentration of stearic acid the protrusions are becoming overlapped and tangled with each other just like S3S. Because of this excessive concentration the empty space/voids between branches are filled with stearic acid. This situation in S2Z4S and S3Z4S can possibly create macroscale roughness that will definitely tune the hydrophobicity. Figure 4.5 (g-h) shows the SEM images of S4Z4S which shows that just like in S4S further increase in concentration of stearic acid to 4wt% the overall microscale roughness is decreasing with protrusions getting wider and distant as compared to S1Z4S, S2Z4S and S3Z4S. The possible reason can be the too much concentration because of which at some places the channels between the protrusions got filled with stearic acid itself making it smooth. In other words because of multilayers of stearic acid the protrusions of layers got interlocked making it smooth that will definitely reduce its hydrophobicity. Anyhow, the scanning electron microscopic analysis conformed that stearic acid have been well coated on sponge surface, without damaging its three dimensional skeleton. As scanning electron microscopy is a surface technique, the presence of ZIF-8 cannot be checked by this technique as it is embedded under the dense layer of stearic acid. The presence of ZIF-8 in this category of samples was checked by FTIR and analyzed.

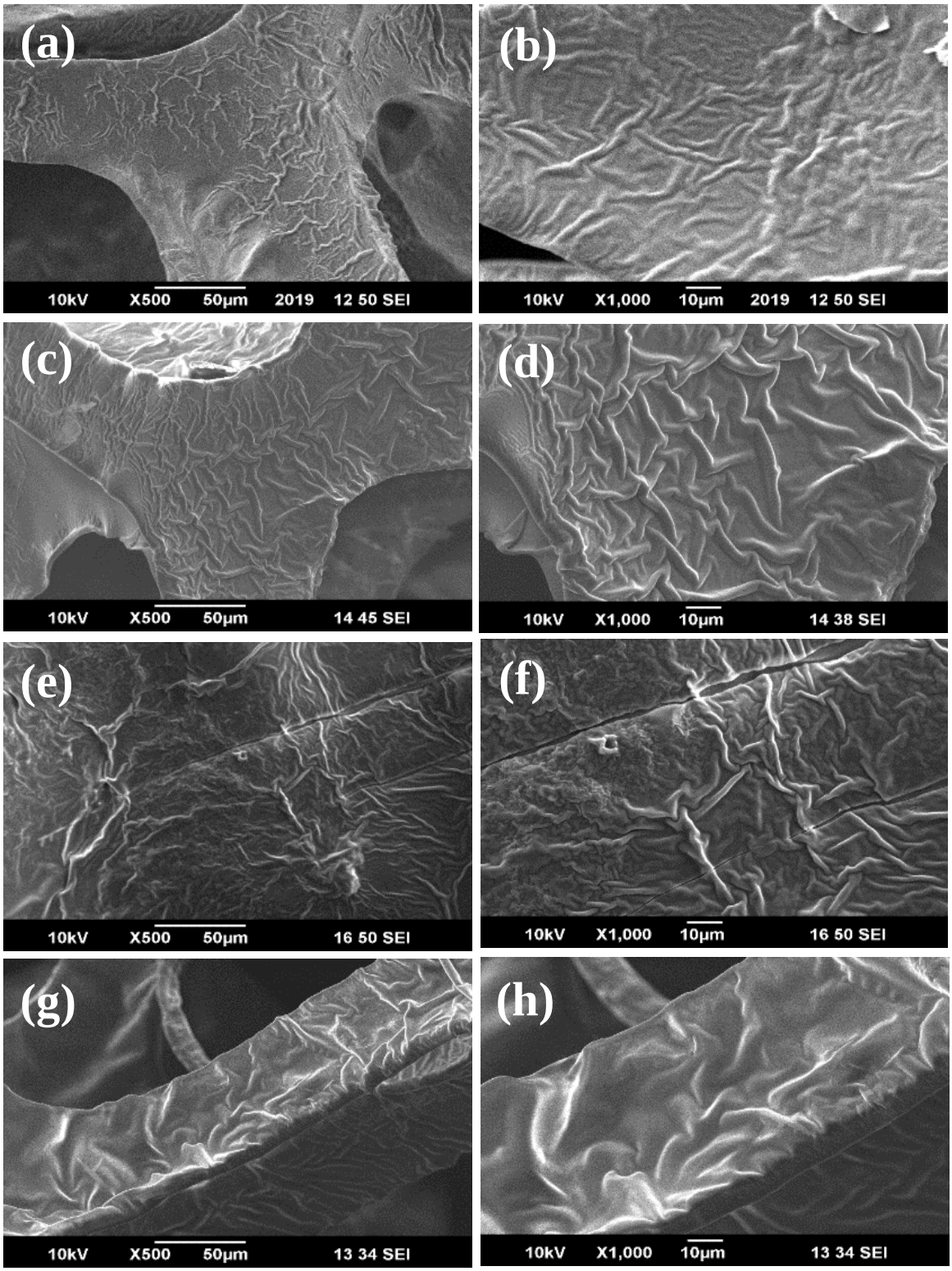

Figure 4. 5 SEM images of (a-b) S1Z4S, (c-d) S2Z4S, (e-f) S3Z4S, (g-h) S4Z4S at different magnifications

4.2.4. Scanning Electron Microscopic Analysis of ZIF-8 @ SA @ Sponge Sample

Figure 4.6 shows the SEM images of Z4S1S composite sponge which is other way round of S1Z4S. Here, the outer layer is ZIF-8 rather than stearic acid, which was observed at higher magnifications. It can be seen clearly from figure 4.6 (a) that ZIF-8 layer is patchy and was not able to cover the sponge uniformly during in-situ growth of ZIF-8, even though concentration used to grow ZIF-8 was of Z4S that forms a uniform layer on sponge skeleton as shown in figure 4.3 (j-l). Evidence of bubble collapse, circled in figure 4.6 (b) can be seen at higher magnification. Knowing the fact that long chain of stearic acid is soluble in organic solvents and polar head that is carboxyl group can easily lose its hydrogen to compounds containing hydroxyl group, it can be concluded that possibly stearic acid after coming in contact with ZIF-8 precursors solution got dispatched from its place [91]. The long chain dissolved in methanol and carboxyl group lost its hydrogen forming water molecule and rest of carboxyl group i-e carbonyl and one oxygen of hydroxyl group seeped out of the ZIF-8 layer in the form of carbon gas. Furthermore, no protrusions of stearic acid are now visible on sponge surface, either under ZIF-8 layer and either on empty space on sponge, which shows that stearic acid layer have been definitely dispatched from the sponge and is unstable in ZIF-8 precursor solutions. So successful formation of this proposed composite i.e. ZIF-8 @ SA @ sponge is impossible in this way. However, to conform its chemical composition FTIR was performed and analyzed.

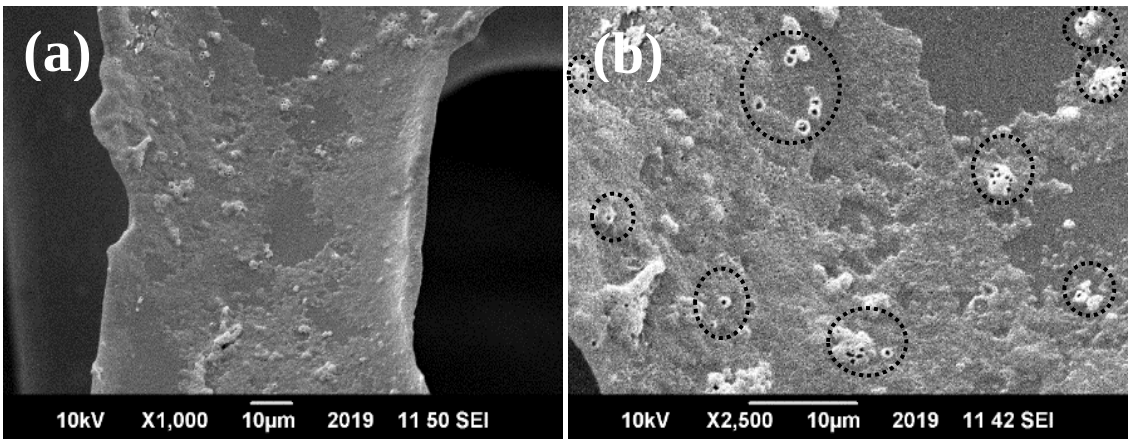

Figure 4. 6 SEM images of Z4S1S at different magnifications

4.2.5. Scanning Electron Microscopic Analysis of SA @ SA @ ZIF-8 @ Sponge Sample

Coating another layer of stearic acid on SA @ ZIF-8 created a well packed structure that is shown in figure 4.7 at different magnifications. The protrusions of stearic acid that is the outer most layer in this composite (S1S1Z4S) sponge can be clearly seen wrapping the entire branch in figure 4.7 (a) At higher magnifications the rough pattern of protrusions can be seen in figure 4.7 (b-c). Here it can be seen that the channels between protrusions are not smooth like in SA @ sponge and SA @ ZIF-8 @ sponge samples. Some thing can been seen popping their heads out of stearic acid layer. These are the protrusions of first layer of stearic acid, increasing the roughness that will definitely contribute in favor of hydrophobicity.

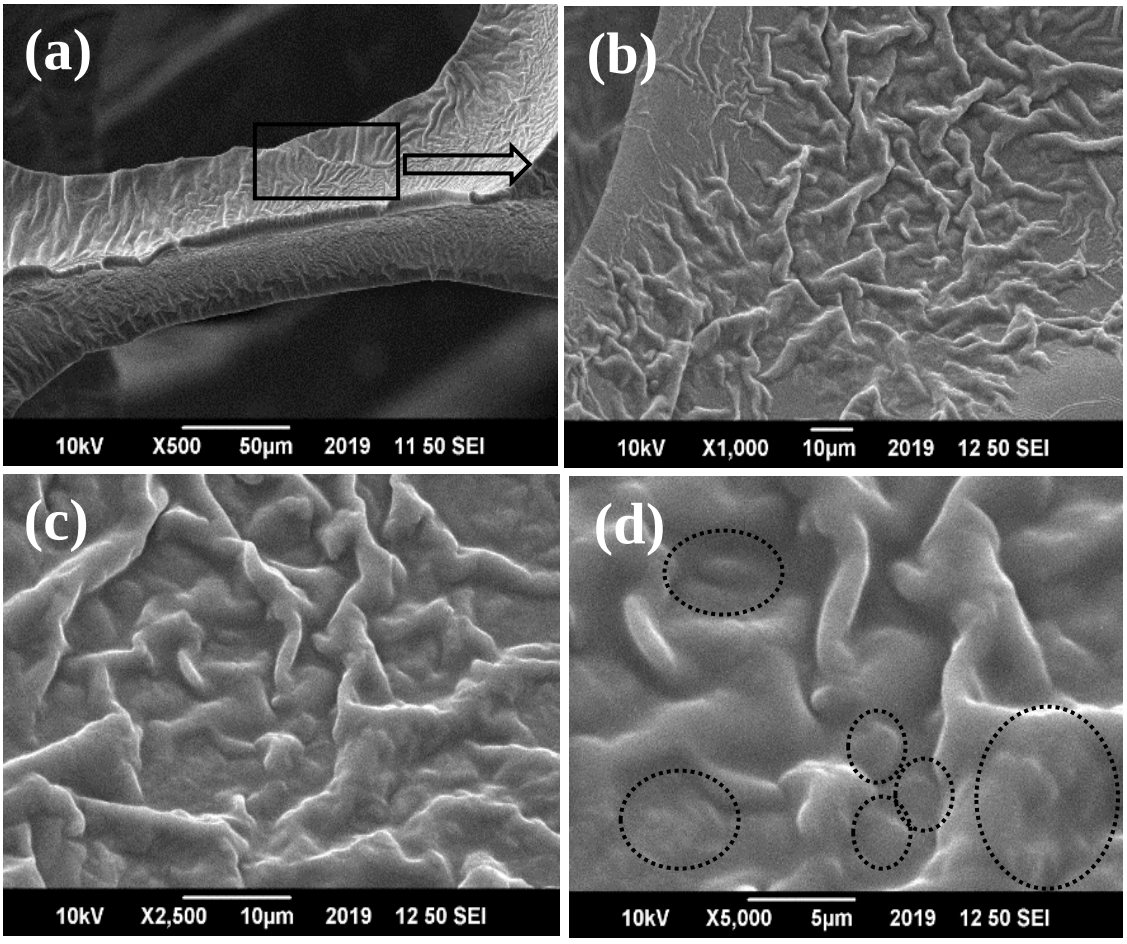

Figure 4. 7 SEM images of S1S1Z4S at different magnifications

4.3. Fourier Transmission Infrared Spectroscopic Analysis

FTIR spectra of pristine sponge, Z4S, S1S, S1Z4S, Z4S1S and S1S1Z4S are shown in figure 4.8. The FTIR spectra of pristine polyurethane sponge shown in figure 4.8 (a) is consistent with that available in literature [87]. The broad band at 3401 cm^{-1} is because of stretching vibrations of N-H, in urethane linkage of polyurethane and the peak at around 2900 cm^{-1} can be correlated to C-H bonds [92]. The peak at around 2324 cm^{-1} can be assigned to the asymmetric stretching of – NCO [82]. The peaks at 1626 cm^{-1}, 1100 cm^{-1} and at 1542 cm^{-1} can be attributed to C = O stretching in urea, ether and amide II band respectively [93]. All these functional groups present in pristine polyurethane sponge are responsible for high polarity and high surface energies that endow it with highly hydrophilic property. The FTIR spectra of Z4S is shown in figure 4.8 (b). The peaks at 2907 cm^{-1}, 1627 cm^{-1} and 1110 cm^{-1} are characteristic peaks of ZIF-8 [94]. The peaks at around these wavelengths (2896 cm^{-1}, 1626 cm^{-1} and 1100 cm^{-1}) are also present in spectra of polyurethane sponge and overlapping of peaks in pristine polyurethane sponge and ZIF-8 caused change in the appearance and wavelengths as compared to pristine polyurethane sponge. The existence of peak at 2907 cm^{-1} is because of stretching vibrations of aliphatic C-H stretch of imidazole [23]. The weakening of this C-H stretch as compared to that of pristine sponge is also a proof of low polarity and less surface energy of Z4S. The peaks at 1627 cm^{-1} and 1110 cm^{-1} are because of vibrations of C=N and C-N respectively [94]. However, a slight change in appearance of broad band between 3000 cm^{-1} to 3500 cm^{-1} is also because of overlapping of N-H stretching vibrations of residual imidazole, water in KBr and N-H in urethane linkage [95]. Some functional groups that were at wavenumber less than 1600 cm^{-1} in pristine sponge, are absent in FTIR Spectra of Z4S, resulting in its less surface energies. This analysis shows that ZIF-8 have interactions with some functional groups present in pristine polyurethane sponge and some new coordination bonds are being formed during in-situ coating process without damaging the backbone of polyurethane in pristine polyurethane sponge and the development of characteristic peaks of ZIF-8 in spectra of Z4S is a proof that ZIF-8 have been successfully grown on sponge skeleton. Figure 4.8 (c) shows the FTIR spectra of S1S. The characteristic peaks of polyurethane at 3364 cm^{-1}, 2326 cm^{-1}, 1228 cm^{-1} and 1100 cm^{-1} can be clearly seen in spectra of S1S with slight peak shifts as compared to original polyurethane sponge , which shows that its structure is still intact after coating it with stearic acid. The change

in appearance of broad band at around 3000 to 3400 cm^{-1} shows that stearic acid have interacted with N-H in urethane linkage. The absence of peaks at 2896 cm^{-1}, 1626 cm^{-1} and 1542 cm^{-1} shows that some functional groups present in pristine polyurethane sponge have made new bonds with stearic acid thus decreasing the polarity of this composite. The peaks at 2916 cm^{-1}, 2852 cm^{-1}, 1701 cm^{-1} and 1442 cm^{-1} are characteristic peaks of stearic acid . The peak at 2916 cm^{-1} and 2852 cm^{-1} can be attributed to anti symmetric and symmetric stretching vibrations of $–CH_2$. The peak at 1701 cm^{-1} is because of C=O stretching vibrations of carboxyl group while the peak at 1442 cm^{-1} can be assigned to $–CH_2$ scissoring vibrations [96]. The presence of characteristic peaks of polyurethane and stearic acid in S1S shows that stearic acid have been successfully coated on it without damaging its structure. FTIR spectra of S1Z4S is shown in figure 4.8 (d). The characteristic peaks of all three components in this composite are visible in its spectra. The peaks at 2311 cm^{-1}, 1642 cm^{-1}, 1536 cm^{-1}, 1227 cm^{-1}, 1100 cm^{-1} and 1048 cm^{-1} are characteristic peaks of polyurethane and the peaks at 1642 cm^{-1} and 1100 cm^{-1} can also considered as the characteristic peaks of ZIF-8 [94] with slight peak shifts as compared to pristine polyurethane sponge used in this work. The peaks at 2917 cm^{-1}, 2854 cm^{-1}, 1705 cm^{-1} and 1432 cm^{-1} are characteristic peaks of stearic acid as described above in case of S1S [96]. Comparing the FTIR spectra of S1Z4S1 with FTIR spectra of Z4S and S1S, of which it is composed of, it can be seen that the broad band at around 3400 cm^{-1} is neither too steep nor too shallow. As described above, the presence of ZIF-8 made this broad band way too steep than pristine polyurethane sponge because of residual imidazole in Z4S and in SIS this broad band is shallow because of interactions of stearic acid with N-H in urethane linkage. The intermediate depth of this broad band in S1Z4S can possibly explain the presence of both ZIF-8 and stearic acid in coated layer. Figure 4.8 (e) shows the FTIR spectra of Z4S1S. Here the characteristic peak of stearic acid at 1705 cm^{-1} because of C = O stretching vibrations of carboxyl group is absent. This result is consistent with its SEM result that shows evidences of bubble collapse because of carbon dioxide seeping out of ZIF-8 layer, formed from on the breakdown of carboxyl group in organic solvent. The peaks at 2922 cm^{-1} and 2855 cm^{-1} are because antisymmetric and symmetric stretching vibrations of $–CH_2$ while the peak at 1452 cm^{-1} is because of $–CH_2$ scissoring vibrations in long chains of residual stearic acid [96]. The characteristic peaks of ZIF-8 are also absent in this spectra of illustrating that it is not successfully grown on sponge surface. The appearance of new peak at 1375 cm^{-1} and absence of some characteristic

peaks of polyurethane, stearic acid and ZIF-8 conforms the presence of new bonds and destructions of old bonds. This analysis together with SEM results shows that the proposed composite (Z4S1S) is not successfully fabricated. Figure 4.8 (f) shows the FTIR spectra of S1S1Z4S. The components of this composite are same in same order as S1Z4S with exception of additional layer of 1 wt% of stearic acid that's why the spectra of this composite is showing the same behavior as S1Z4S. The characteristic peaks off all three components are present in its spectra which shows that the sample have been successfully fabricated as desired without damaging the sponge skeleton.

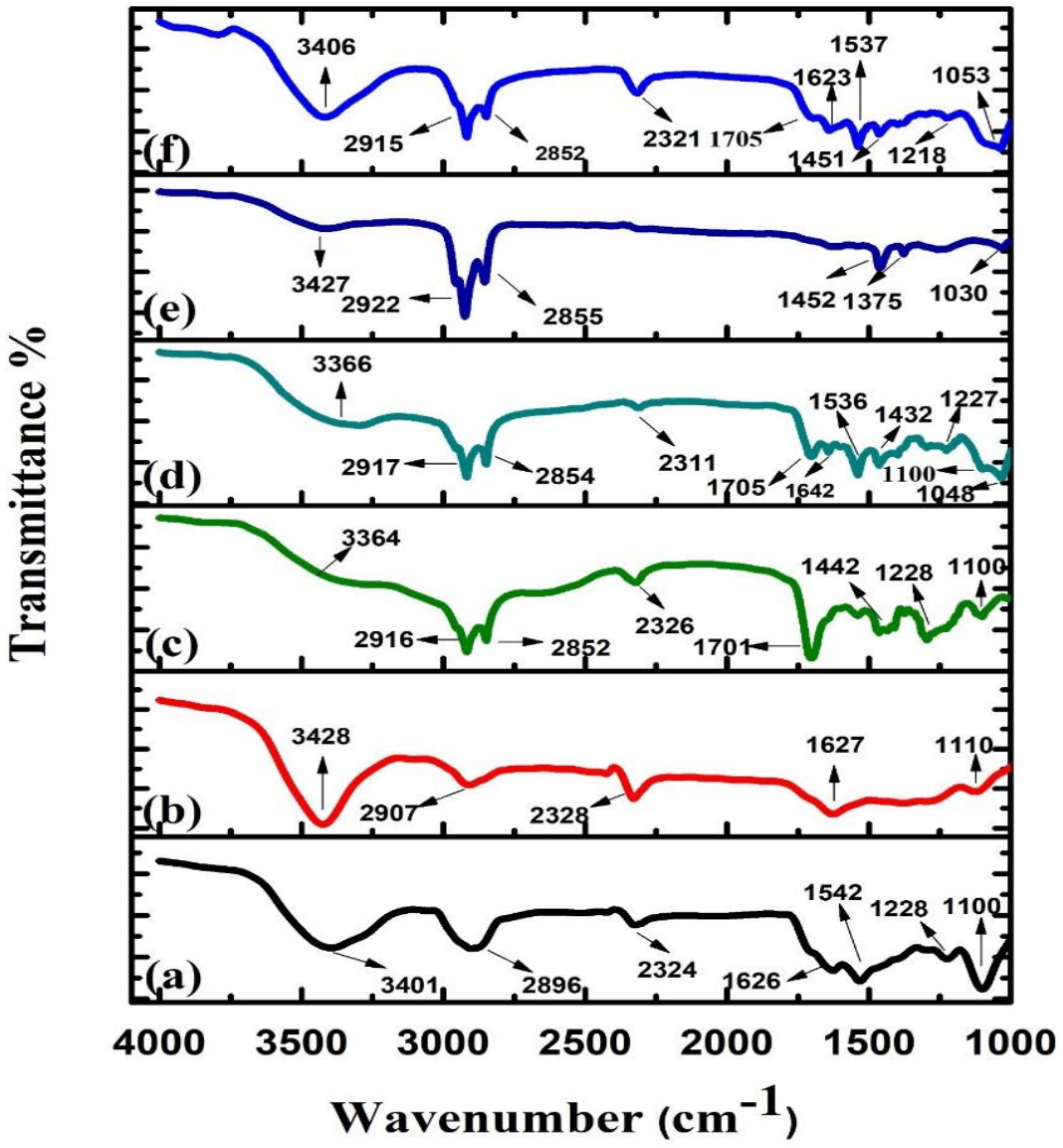

Figure 4. 8 FTIR spectra of (a) pristine sponge, (b) Z4S, (c) S1S, (d) S1Z4S, (e) Z4S1S, (f) S1S1Z4S

4.4. Hydrophobic and Lipophilic Analysis

4.4.1. Hydrophobic and Lipophilic Analysis of pristine sponge

The left and right water contact angles (WCAs) of pristine and ZIF-8 coated sponges are shown in figure 4.9. The pristine sponge used in this work exhibited a WCA of 88.8º proving it a hydrophilic material. Considering surface roughness and chemical composition of material as two main factors for achieving hydrophobicity, this can be ascribed to the presence of highly polar functional groups that were diagnosed in its FTIR spectra and a very smooth and clear branch's surface that was found in its SEM images.

4.4.2. Hydrophobic and Lipophilic Analysis of ZIF-8 @ Sponge Samples

When pristine sponge was coated with different loadings of ZIF-8, the WCA gradually increased to a certain extent and then decreased as shown in figure 4.10. Z1S showed a slight increase of 2.4º in WCA as compared to pristine sponge. This can be attributed to very less growth of ZIF-8 on sponge's surface, as shown by its SEM images. Z2S showed, not significant but higher hydrophobicity (WCA= 100º) than Z1S. This increase can also be correlated to its SEM results that showed more ZIF-8 particles adhered on the surface. On further increase in loading, a significant difference of 18° between the hydrophobicity of Z2S (WCA = 100º) and Z3S (WCA= 118.1º) was observed. This can be accredited to good enough coverage of ZIF-8 particles on the surface of sponge. Nevertheless, Z4S exhibited highest WCA of 129.2° among all ZIF-8 @ Sponge samples. The difference in hydrophobicity of Z3S and Z4S can be credited to coated film, that was patchy and fractured in Z3S, endowing it with macroscale roughness while it was neither patchy nor fractured but uniform and entirely covering the branches of sponge in Z4S, endowing it with microscale roughness. Also, because of this entire coverage of ZIF-8 on surface, polarity of pristine sponge decreased, leading to decreased surface energies that was confirmed by its FTIR spectra. On further increase in concentration to Z5S, an interesting decline in hydrophobicity was observed. This is because of agglomerations of ZIF-8 particles because of rapid nucleation and growth at too much high concentration. These results are consistent with the results of Setareh Salehabadi et al [97]. Furthermore, when a droplet of oil was dropped on the surface of Z4S, it was immediately completely absorbed, giving an oil contact angle (OCA) of 0º. Figure 4.11 shows the optical images of water droplet, dyed with methyl orange and diesel droplet completed absorbed in surface.

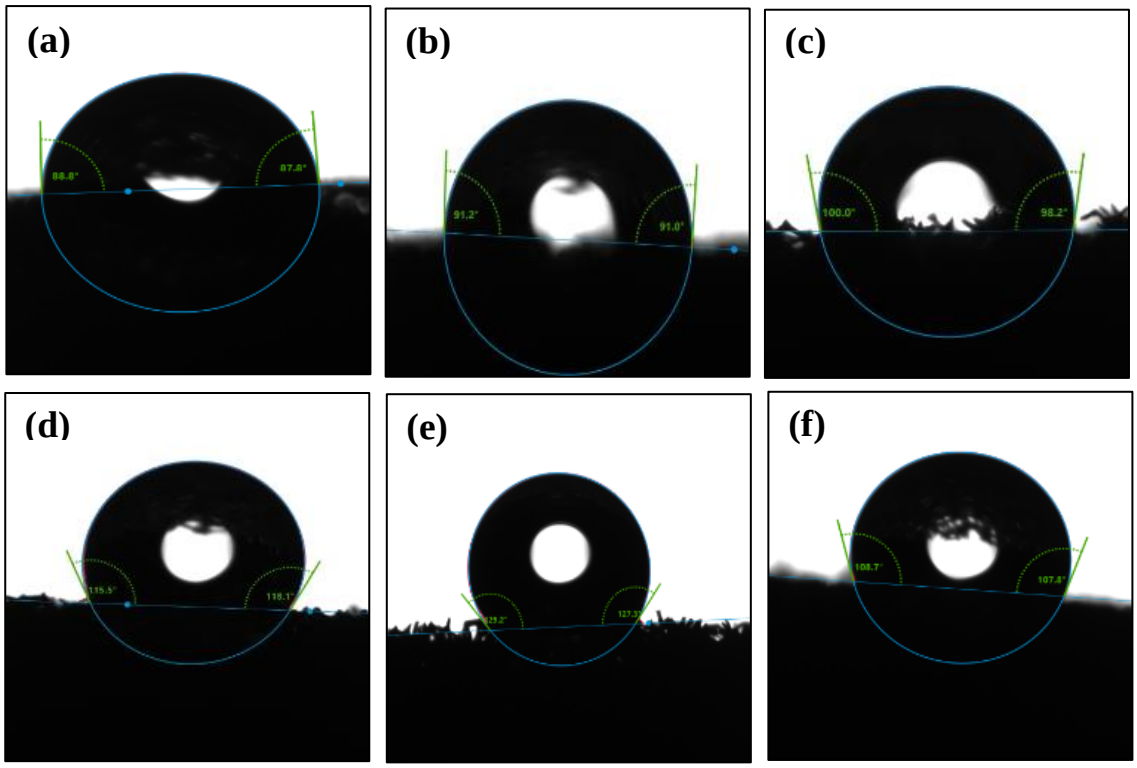

Figure 4. 9 Contact angles of (a) Pristine sponge, (b) Z1S, (c) Z2S, (d) Z3S, (e) Z4S, (f) Z5S

Table 4. 1 Relationship between reactants ratio, loading ratio % and contact angle of PS and ZIF-8 @ Sponge samples

Sample	**Zn^{+2} :Hmim: MeOH (molar ratio)**	**Loading ratio %**	**Water Contact Angle**
PS	0 :0.00: 000.00	0.00	088.8°
Z1S	1 :8.08: 499.75	1.90	091.2°
Z2S	1 :8.08: 249.87	3.46	100.0°
Z3S	1 :8.08: 166.58	5.01	118.1°
Z4S	1 :8.08: 124.93	6.26	129.2°
Z5S	1 :8.08: 099.90	7.30	108.7°

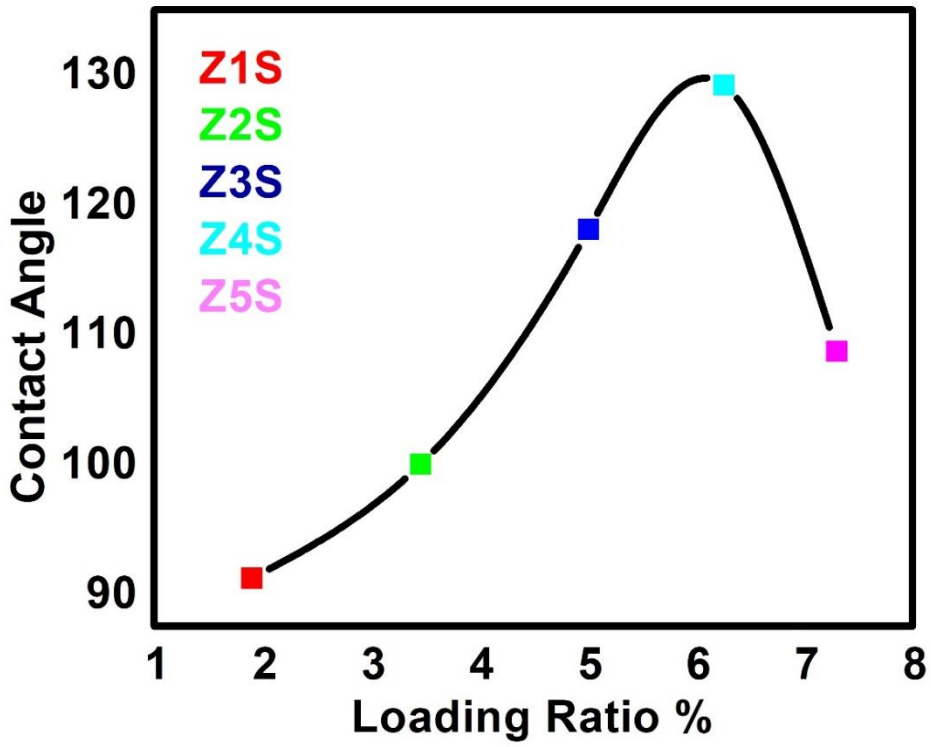

Figure 4. 10 Relationship between loading Ratio % and contact angle of ZIF-8 @ Sponge samples

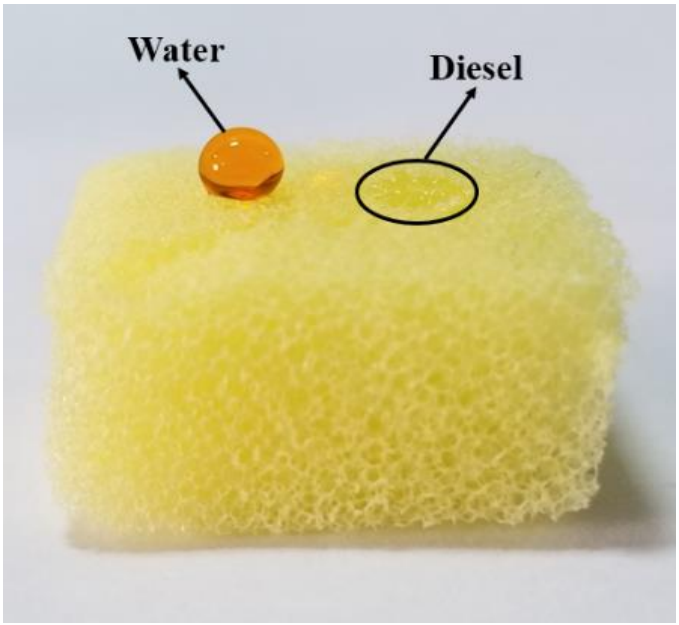

Figure 4. 11 Optical image of water droplet (dyed orange) and diesel droplet on the surface of Z4S

4.4.3. Hydrophobic and Lipophilic Analysis of SA @ Sponge samples

The left and right water contacts angles (WCA) of SA @ sponge samples are shown in figure 4.12. It is observed that the contact angles are decreasing slightly with increase in concentration of stearic acid. S1S exhibited highest contact angle of 139.3° among this category of samples, shown in figure 4.12 (a). Considering chemical composition

and surface roughness as main factors to achieve hydrophobicity this can be attributed to the proposed mechanism of stearic acid absorption on sponge surface which states that the polar end that is carboxyl group makes new bonds with sponge surface as described in its FTIR spectra and gets attach to sponge surface with long non polar tail facing outwards (figure 4.11) that enrich it with low surface energy and uniform wrinkled pattern of coated layer as observed in its SEM images that endue it with good enough roughness to gain this hydrophobicity. On further increase in concentration to 2wt% and 3wt% the contact angle of S2S decreased by 3° giving a value of 136.4° and contact angle of S3S decreased by 5.6° giving a value of 133.7° , shown in figure 4.12 (b, c). The one obvious reason as described in its SEM images is the morphology of coated layer in which the protrusions are stronger, heightened and tangled in S2S than S1S and in S3S than S2S. This condition is responsible for creating macroscale roughness and obviously a decrease in hydrophobicity. Figure 4.12 (d) shows that the contact angle of S4S is 130.8° which is least among all in this category of samples. This can be attributed to its smooth surface formed because of interlocking of protrusions at too much high concentration as already described in its SEM results. Possible second reason is that because of excess concentration of stearic acid, the non-polar / non-polar attractions, between the long alkyl chains of stearic acid molecules attaching first on the surface sponge with long alkyl chains of remaining molecules of stearic acid, come into play that causes exposure of polar ends of stearic acid molecules to surface thus increasing the surface energy and decreasing the hydrophobicity [98]. So, it can be said that higher the concentration of stearic acid more are the non-polar / non-polar attractions because of excessive molecules of stearic acid available so more is the decline in contact angle that's why contact angle of S4S < S3S < S2S <S1S. The proposed mechanism of stearic acid adsorption on sponge surface is shown in figure 4.14. Moreover, when a drop of oil is place on the surface of S1S it was immediately absorbed. Figure 4.13 shows the optical image of S1S after treating it with water and diesel oil. The water droplet dyed orange maintains its circular shape while the diesel droplet was absorbed immediately leaving a wet surface behind.

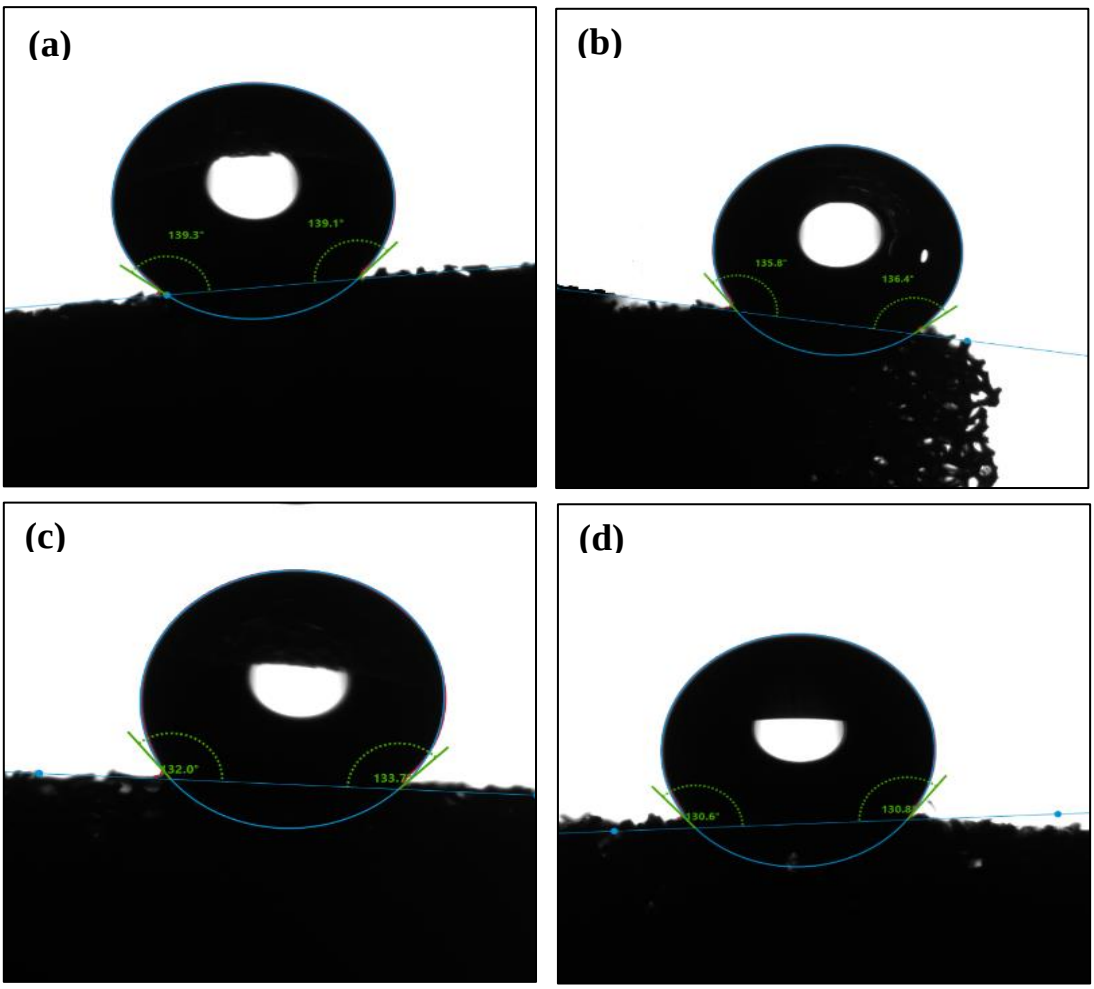

Figure 4. 12 Contact angles of (a) S1S, (b) S2S, (c) S3S, (d) S4S

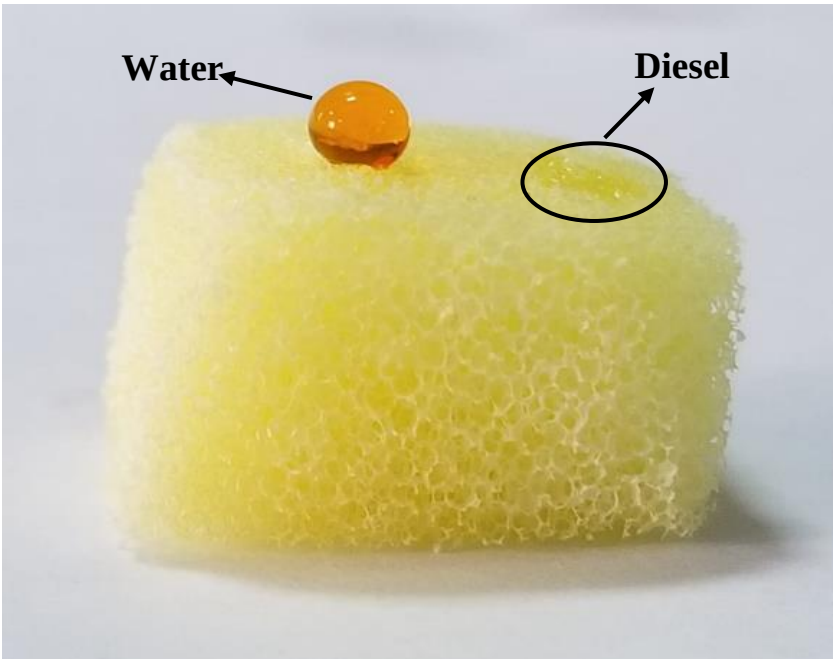

Figure 4. 13 Optical image of water droplet (dyed orange) and diesel droplet on the surface of S1S

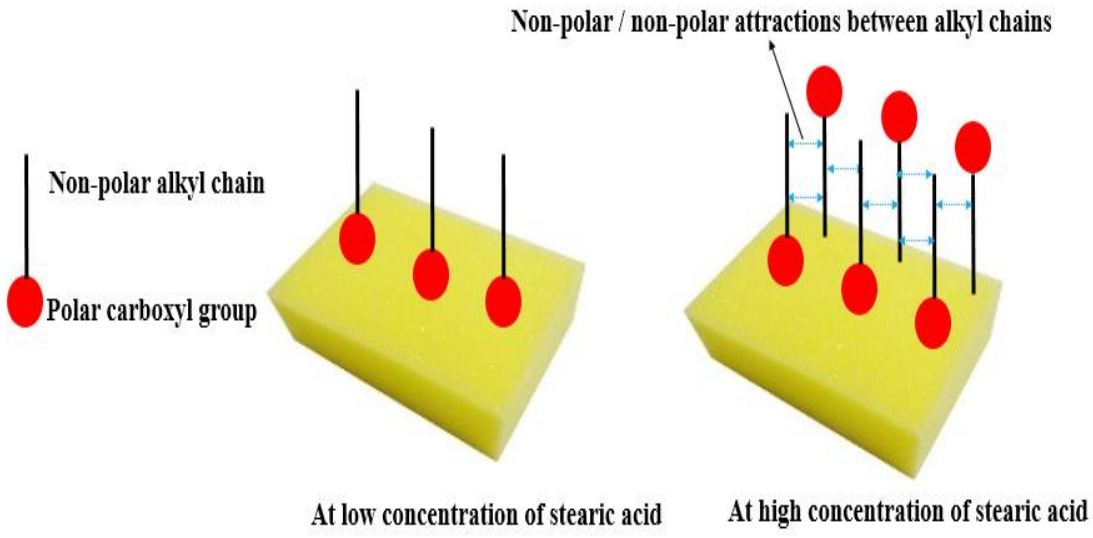

Figure 4. 14 Mechanism of stearic acid adsorption on sponge surface at different concentrations

4.4.4. Hydrophobic and Lipophilic Analysis of SA @ ZIF-8 @ Sponge Samples

The left and right water contact angles of all samples of SA @ ZIF-8 @ Sponge are shown in figure 4.14. It is observed that the contact angles are decreasing with increase in concentration of stearic acid just like SA @ Sponge samples because here the outer layer is also stearic acid and is in same concentration as in SA @ Sponge. S1Z4S showed highest contact angle of 140.8° represented in figure 4.15 (a) while S2Z4S, S3Z4S and S4Z4S showed contact angles of 137.9°, 134.9° and 131.2° respectively as shown in figure 4.15 (b, c and d respectively) As already described in SEM results morphologically S1Z4S is congruent with S1S, S2Z4S is congruent with S2S, S3Z4S is congruent with S3S and S4Z4S is congruent with S4S so, decreasing contact angles by increasing the concentration of stearic acid can be also explained by section 4.4.3. However, a small increase of about 1° to 1.5° in contact angle of every SA @ ZIF-8 @ sponge as compared to its corresponding SA @ Sponge sample is possibly because of ZIF-8 present in them. As presence of ZIF-8 is not much effecting the hydrophobicity in this composite, considering ZIF-8 a highly porous material and good absorbent, the effect of ZIF-8 on absorption capacity was checked which will be explained later in the chapter. Moreover, when a diesel droplet was placed on the surface of S1Z4S it was immediately absorbed while water droplet maintains its circular shape as shown in figure 4.16.

Table 4. 2 Comparison of WCAs of SA @ Sponge and SA @ ZIF-8 @ Sponge samples

SA @ Sponge	WCA	SA @ ZIF-8 @ Sponge	WCA	Difference of corresponding WCAs
S1S	139.3°	S1Z4S	140.8°	1.5°
S2S	136.6°	S2Z4S	137.9°	1.3°
S3S	133.7°	S3Z4S	134.9°	1.2°
S4S	130.8°	S4Z4S	131.8°	1°

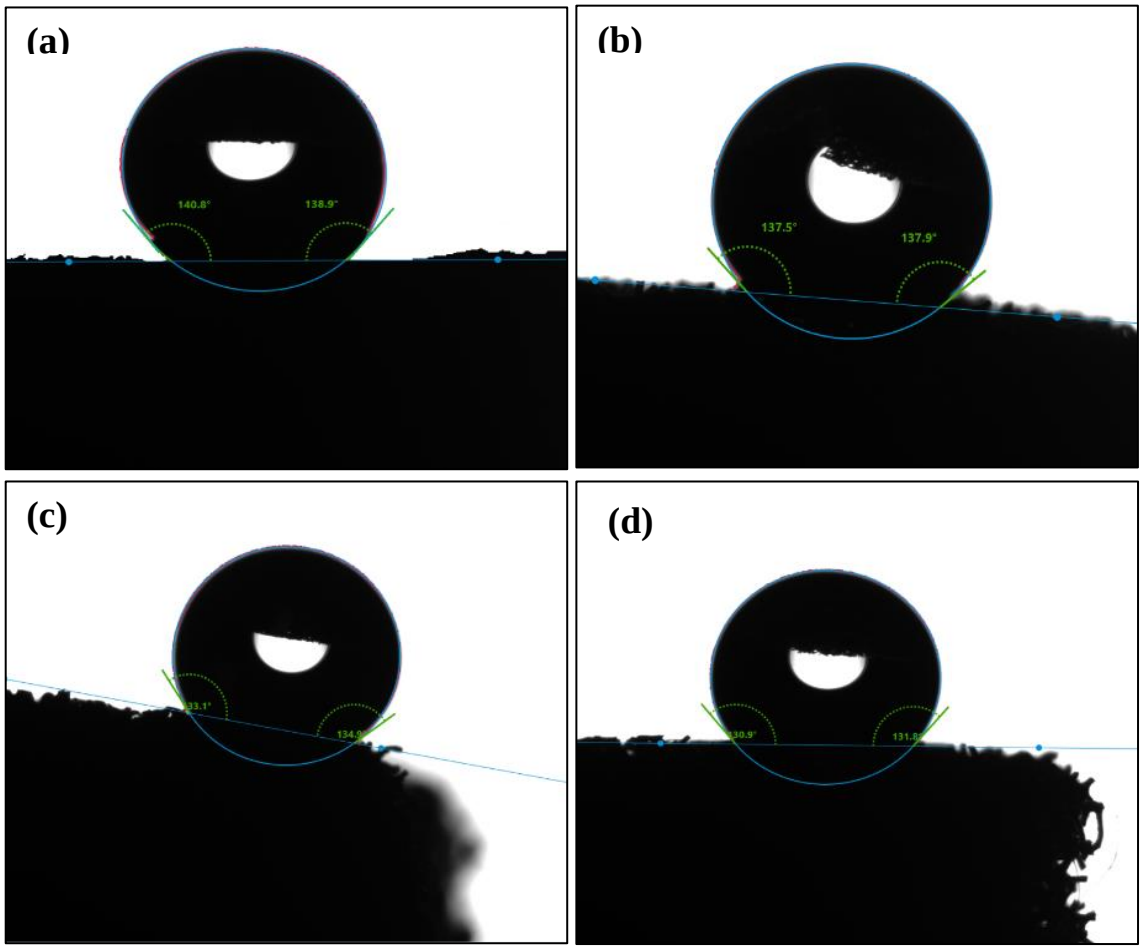

Figure 4. 15 Contact angles of (a) S1Z4S, (b) S2Z4S, (c) S3Z4S, (d) S4Z4S

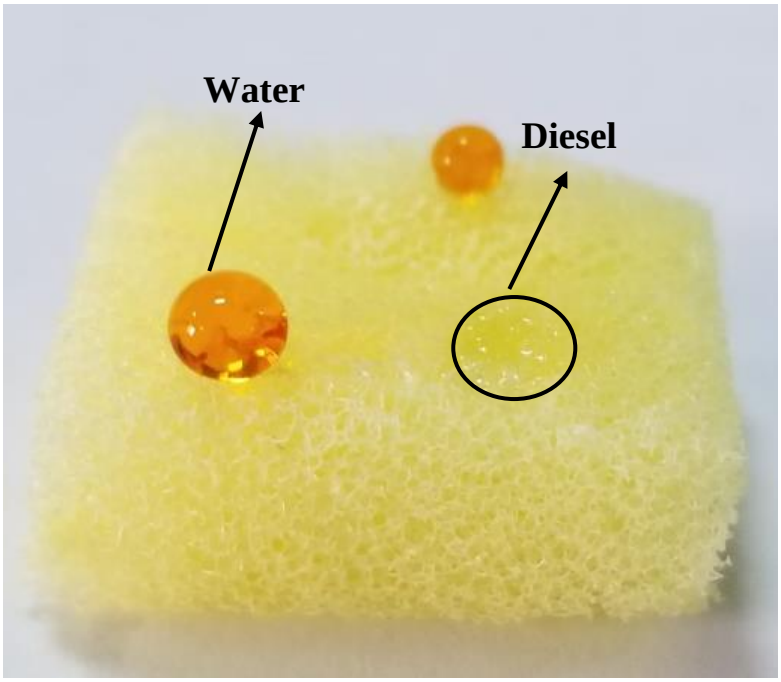

Figure 4. 16 Optical image of water droplet (dyed orange) and diesel droplet on the surface of S1Z4S

4.4.5. Hydrophobic and Lipophilic Analysis of ZIF-8 @ SA @ Sponge Sample

The left and right water contact angle of ZIF-8 @ SA @ sponge is shown is figure 4.17. Figure 4.17 shows that the contact angle of Z4S1S is 110.7°. This drastic decrease in contact angle of Z4S1S as compared to other composites of stearic acid can be correlated to its SEM and FTIR results which shows that stearic acid layer got dispatched from the surface after coming in contact with ZIF-8 precursor solutions during in-situ synthesis of ZIF-8, also effecting the formation of ZIF-8. In fact proposed composite neither have stearic acid nor ZIF-8 present in it according to its SEM and FTIR analysis so decrease in its hydrophobicity is certain and not surprising. Moreover, when a drop of diesel and water was placed together on the surface of sponge for optical analysis it was observed that diesel immediately absorbed in it and water droplet also lost its shape from circular to semicircular immediately after comping in contact with its surface and was completely absorbed after 30s.

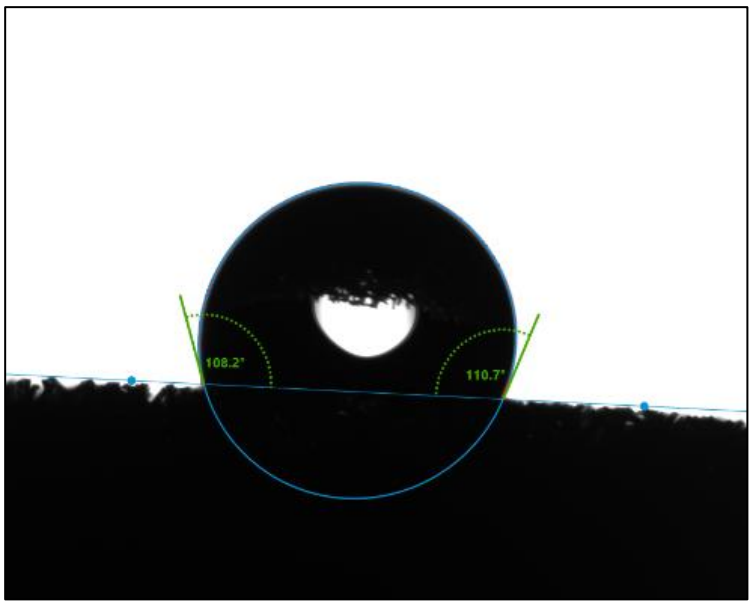

Figure 4. 17 Contact angle of Z4S1S

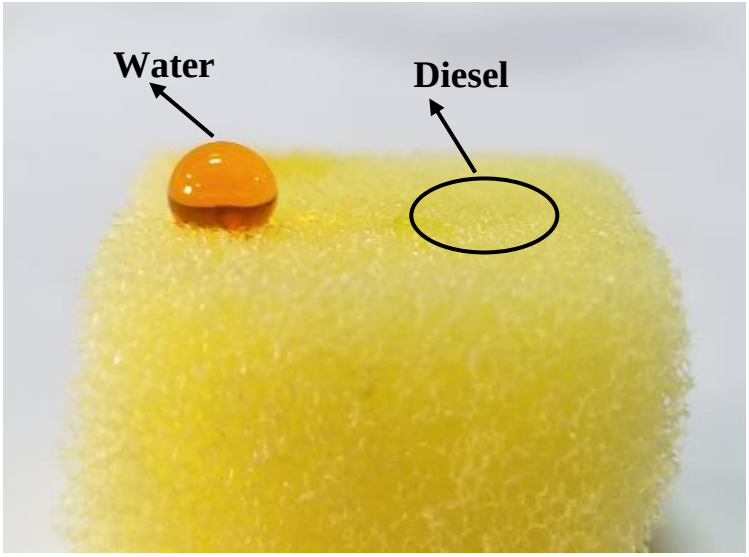

Figure 4. 18 : Optical image of water droplet (dyed orange) and diesel droplet on the surface of Z4S1S

4.4.6. Hydrophobic and Lipophilic Analysis of SA @ SA @ ZIF-8 @ Sponge Sample

Realizing that SA @ ZIF-8 @ sponge is highly hydrophobic composite giving a contact angle of 140° another layer with 1wt% stearic acid is coated on S1Z4S to get layer by layer coating of stearic acid on sponge. The low concentration of stearic acid is chosen here because at higher concentrations the non-polar / non-polar attractions cause exposure of polar ends to the surface thus decreasing the hydrophobicity as shown in figure 4.14. S1S1Z4S showed same FTIR pattern as S1Z4S because of same chemical components present in them however, the second layer of stearic acid caused a little bit increase in roughness as described in its SEM results. That's why its contact angle showed a small increase of about 2.5° giving the equal left and right contact angle of 143.2° as shown in figure 4.19. Moreover, when a drop of diesel and water is placed together on its surface for optical analysis the diesel droplet is absorbed immediately while water droplet maintains its perfect circular shape as shown in figure 4.20.

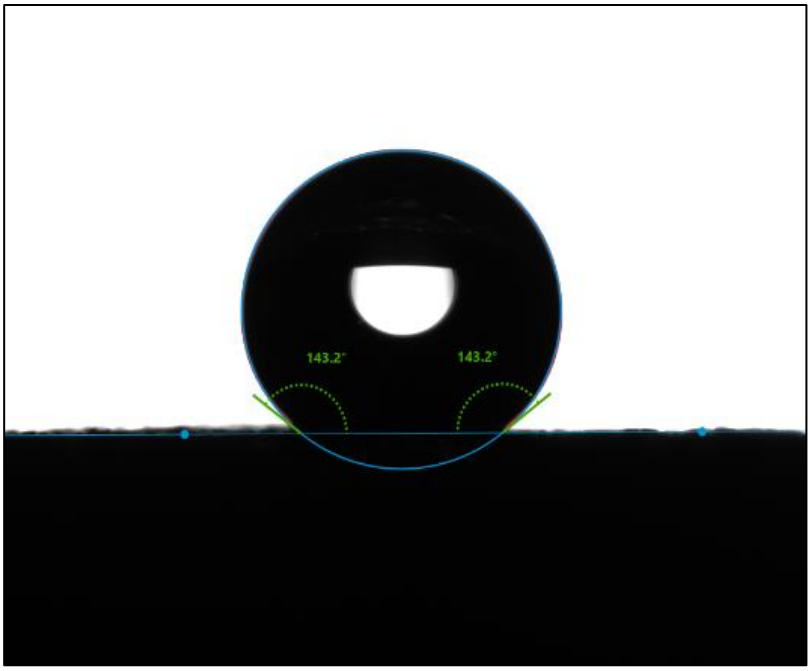

Figure 4. 19 Contact angle of S1S1Z4S

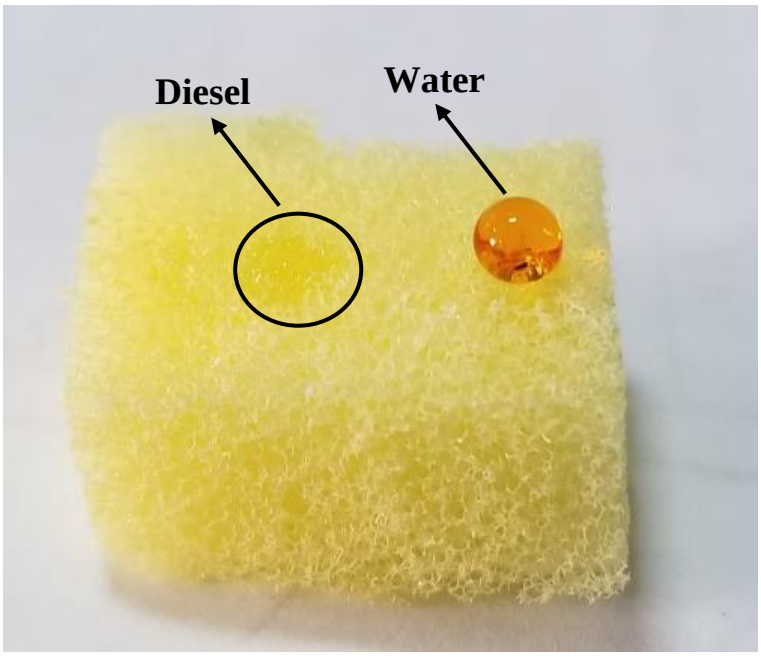

Figure 4. 20 Optical image of water droplet (dyed orange) and diesel droplet on the surface of S1S1Z4S

Figure 4. 21 Optical image of S1S1Z4S under excessive amount of water droplets (dyed orange)

4.5. Absorption Capacity (g/g)

Based on the results of hydrophobic analysis, sample giving highest contact angle from every category is tested for oil/water separation experiment according to the method described in section 3.7 and its absorption capacity is calculated by using equation 3.2. Five type of oil / organic solvents with different the densities, ranging from 850 to 1850

kg/m^3 are chosen. The results of this test are plotted in the form of bar chart shown in figure 4.22. It can be clearly seen from bar chart that chloroform is most absorbed organic solvent in all samples ranging from 43.16 g/g to 115.35 g/g. Depending upon the type of sample, Z4S gave good enough value of absorption capacity for all type of oil / organic solvents ranging from 29.3125 g/g for n-hexane to 79.21 g/g for chloroform. This can be attributed to excellent coverage of ZIF-8 on the surface of sponge in Z4S and obviously porous nature of ZIF-8 which makes it a good absorbent material. Although S1S shows good hydrophobicity (WCA=139.3°) but it gives not so good value of absorption capacity as compared to other samples used for this test ranging from 7.28 g/g for vegetable oil to 43.16 g/g for chloroform. The low value of absorption capacity makes S1S not suitable for large scale practical applications despite of having good hydrophobicity. The absorption capacity of S1Z4S is highest for diesel, petrol, n-hexane and chloroform as compared to the absorption capacity of all other samples used for this test, ranging from 30.26 g/g for n-hexane to 115.35 g/g for chloroform. For vegetable oil it is 40.23 g/g that is a little smaller than the absorption capacity of Z4S for vegetable oil (41.736 g/g). So it can be said that incorporation of ZIF-8 in S1S to make it S1Z4S increases its absorption capacity to a good extent. The absorption capacity of Z4S1S ranges from 21.36 g/g for n-hexane to 61.33 g/g for chloroform. As already described in SEM and FTIR results that the stearic acid layer gets dispatched from surface after coming in contact with ZIF-8 precursor solutions and formation of ZIF-8 is not successful in Z4S1S because of which it is not hydrophobic. It can absorb oil as shown in figure 4.18 but its absorption capacity in grams of oil absorbed per grams of sponge is very low because there is no ZIF-8 present in it as it was not even formed. . Being a bad hydrophobic composite with less absorption capacity it is certainly not fit for large even small scale applications. Unexpectedly absorption capacity of S1S1Z4S decreased as compared to S1Z4S ranging from 17 g/g for vegetable oil to 58.656 g/g for chloroform. Because of layer by layer coating of stearic acid it gives highest contact angel but double layers of stearic acid create an effect like S1S that's why the value of its absorption capacity is about that of S1S. These values are comparable to or more than the values already available in literature (Table 2.1). On the basis of these results it can be concluded that S1Z4S is an optimum material for practical application with high hydrophobicity and good absorption capacity.

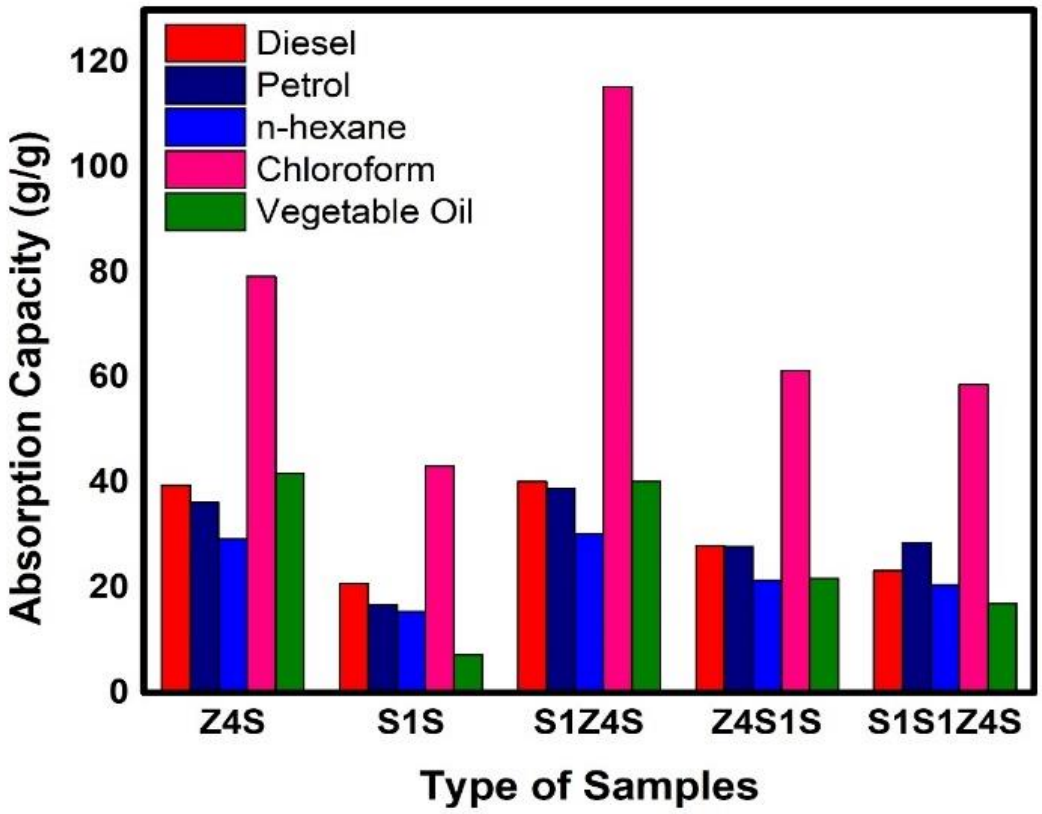

Figure 4. 22 Absorption capacity of Z4S, S1S, S1Z4S, Z4S1S and S1S1Z4S for different type of oil / organic solvents

4.6. Recyclability

As recyclability and reusability as an important factor for practical application, recyclability test for Z4S and S1Z4S is performed according to the method described in section 3.8. Diesel and chloroform are chosen randomly as test solvents. Z4S and S1Z4S are chosen based on their good absorption capacity. Absorption capacity and collection capacity for every cycle is calculated by using equation 3.2 and 3.3 respectively. The results for ten cycles are plotted in the form of graph, shown in figure 4.23 and 4.24. Both Z4S and S1Z4S showed no significant decrease in absorption capacity and no substantial increase in collection capacity for over ten cycles. This can be attributed to the excellent coverage of coating materials on the surface of sponge and chemical attachment of ZIF-8 on sponge surface because of which it can't be desorbed easily. Collection capacity of both Z4S and S1Z4S is high for chloroform as compared to diesel. This is because chloroform is very dense as compared to diesel used for this

test. The high absorption capacity for more than 10 cycles, easy recovery of absorbed oil by simple squeezing / pressing and less collection capacity for over ten cycles shows that Z4S and S1Z4S can be a potential candidates for practical application.

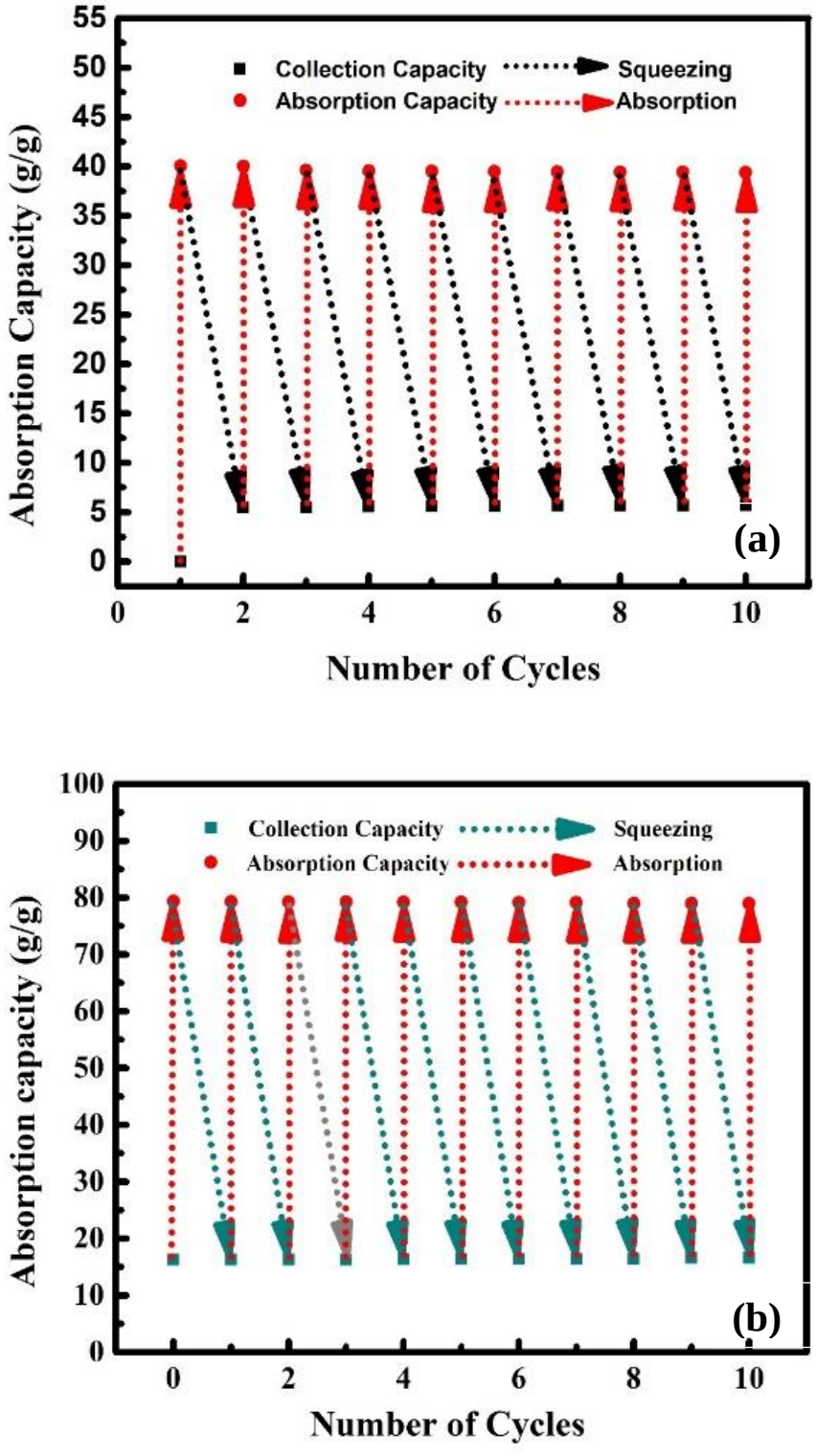

Figure 4. 23 Recyclability of Z4S with (a) Diesel, (b) Chloroform

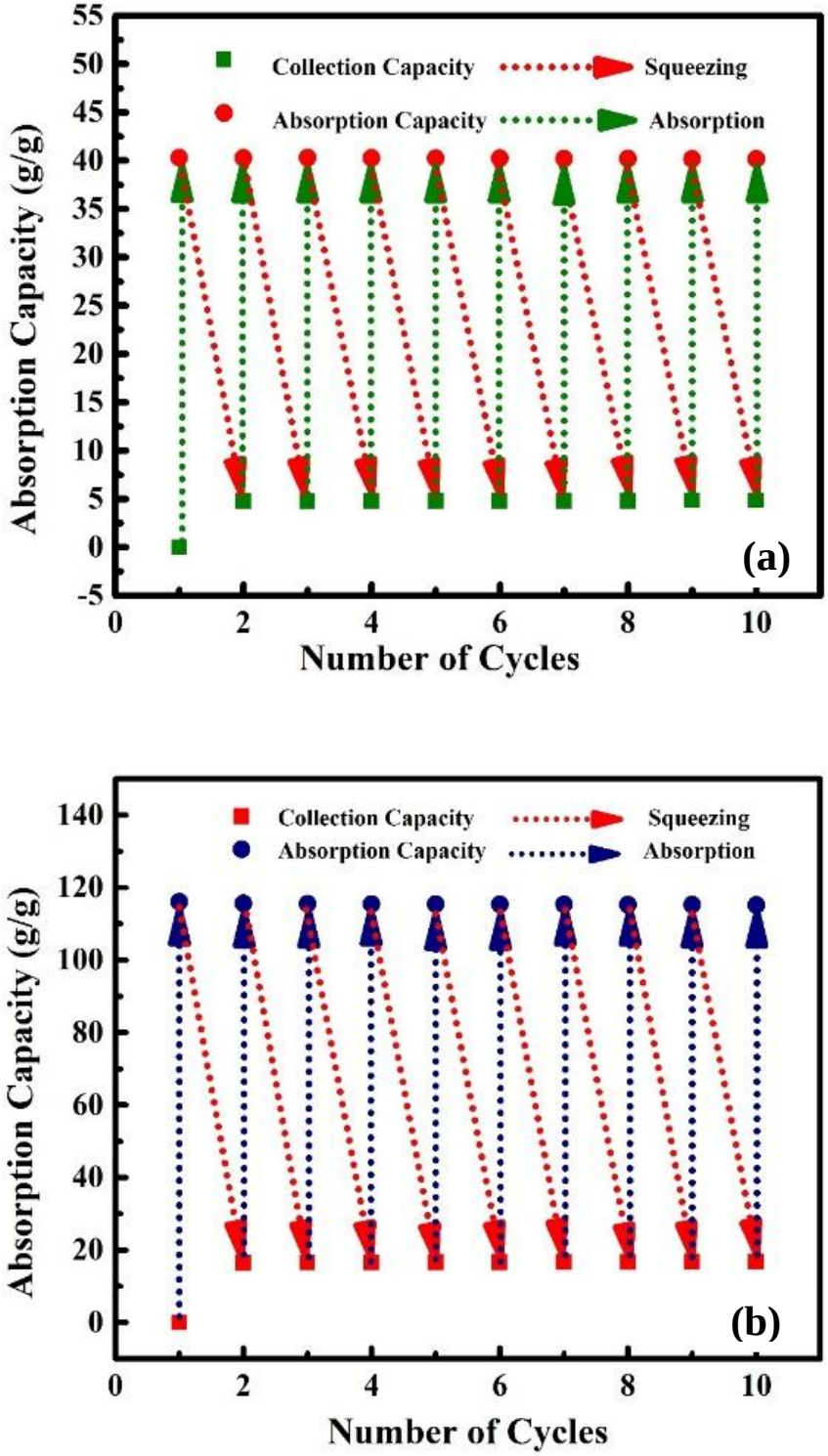

Figure 4. 24 Recyclability of S1Z4S with (a) Diesel, (b) Chloroform

Table 4. 3 Summary of results of tests performed with different samples

Sample	Average Absorption Capacity (g/g)					Average Collection Capacity (g/g)		Rc (cycles)
	Diesel	Petrol	hexane	Chloroform	Vegetable Oil	Diesel	Chloroform	
Z4S	39.5	36.21	29.31	79.21	41.74	5.6	16.4	10
S1S	20.82	16.86	15.48	43.16	7.28	…	…	…
S1Z4S	40.21	38.93	30.26	115.35	40.23	4.8	16.6	…
Z4S1S	27.95	27.81	21.36	61.33	21.77	…	…	10
S1S1Z4S	23.21	28.60	20.56	58.66	17.01	…	…	…

Conclusion

Conclusively, MOF functionalized, stearic acid functionalized and stearic acid @ MOF based hydrophobic polyurethane sponges were successfully fabricated for the first time. In case of MOF functionalized sponges xrd analysis conformed the successful growth of ZIF-8 on sponge skeleton. The effect of concentration of ZIF-8 precursor solutions on coverage of sponge surface was examined by sacnning electron microscopy which showed that changing concentration changes the morphology of ZIF-8 particles as well as the coverage becomes uniform (sample: Z4S) at molar ratio 1:8.08: 124.93 of Zn^{+2}, Hmim and MeOH respectively. Contact angle measurements confirmed that increase in loading doesn't always increases the hydrophobicity. For higher hydrophobicity uniform coating on surface having microscale roughness is necessary. FTIR analysis showed the reduced polarity of Z4S as compared to pristine polyurethane sponge that justifies its high hydrophobicity as compared to Pristine polyurethane sponge. Moverover, Z4S showed good recyclability for over ten cyles and good absorption capacity ranging from 29 to 79 g/g for different oils / organic solvents. So, in case of MOF based sponges ZS4 can be chosen as an optimum candidate for many applications like in oil storgae, cleanup of oil spills and industrial oily water treatment.

In case of stearic acid functionalized and stearic acid @ MOF based sponges it was found that high concentration of stearic acid does not contributes in favor of hydrophobicity firstly, because of non-polar / non-polar attractions between long chains of stearic acid that exposes polar ends outwards and secondly because of uneven surface with macro-bumps forming at high concentration that was found in their SEM images. So further analysis was done only for samples having 1 wt% of stearic acid. Their FTIR analysis conformed the successful growth of stearic acid and stearic acid @ MOF without damaging the sponge skeleton. Furthermore, stearic acid functionalized sponge showed less absorption capacity, ranging from 7.28 to 43.16 times its own weight for different oils / organic solvent, as compared to stearic acid @ MOF based sponge that showed high absorption capacity ranging from 30.26 to 115.35 times its own weight. The high value of absorption capacity of stearic acid @ MOF based sponge can be accredited to high surface area and highly porous nature of ZIF-8 present in it. Moreover, it showed less collection capacity and reusability for over ten cycles. Coating another layer of stearic acid on it caused an increase in hydrophobicity but decrease in absorption capacity possibly because of enfolding of ZIF-8 layer by stearic acid double

layers which makes ZIF-8 pores inaccessible during separation. Moreover, the successful fabrication of MOF functionalized stearic acid sponge (ZIF-8 @ SA @ Sponge) was not possible because stearic acid layer is not stable in organic solvents, dispatches from surface and hinders the successful formation of ZIF-8 which was confirmed by its SEM and FTIR analysis. So, only low concentration stearic acid @ MOF functionalized sponge being a three in one package, utilizing the inherited properties of MOFs i.e. high surface area, controllable pore size and chemical functionality at molecular level, non-wetting / highly hydrophobic property of stearic acid and regular 3D skeleton of highly porous polyurethane sponge , possessing high hydrophobicity, high oil absorption capacity, low collection capacity and excellent reusability can be an optimum candidate for large scale practical application.

Future Recommendations

As this is the first study on stearic acid @ MOF based polyurethane sponge for oil/water separation so there are some important properties that are required to be explored for its full scale application. For example, the oily effluents from different industries contain toxic chemicals and can have varying PH so, a study on stability of proposed sponges under harsh conditions should be conducted. As oil and organic solvents are highly flammable so a study on flame resistance of proposed sponges should be done before use to avoid any accident. Considering that there are thousands of MOFs present, stearic acid can be used to functionalize other MOFs as well to get better results.

References

[1] A. Inyinbor, B. Adebesin, A. Oluyori, T. Adelani-Akande, A. O. Dada, and O. A, "Water Pollution: Effects, Prevention, and Climatic Impact," ed, 2018.

[2] S. Ahuja, "Chapter 1 - Overview: Evaluating Water Quality to Prevent Future Disasters," in *Separation Science and Technology*. vol. 11, S. Ahuja, Ed., ed: Academic Press, 2019, pp. 1-12.

[3] A. Gupta, "WATER POLLUTION-SOURCES,EFFECTS AND CONTROL," *Pointer Publishers Jaipur.*, 01/01 2016.

[4] J. V. Macías-Zamora, "Chapter 19 - Ocean Pollution," in *Waste*, T. M. Letcher and D. A. Vallero, Eds., ed Boston: Academic Press, 2011, pp. 265-279.

[5] M. Cheryan and N. Rajagopalan, "Membrane processing of oily streams. Wastewater treatment and waste reduction," *Journal of Membrane Science,* vol. 151, pp. 13-28, 1998/12/09/ 1998.

[6] J. W. Patterson, *Industrial wastewater treatment technology, Second edition*. United States: Butterworth Publishers,Stoneham, MA, 1985.

[7] M. A. Cohen, "Water Pollution from Oil Spills," *Encyclopedia Energ. Nat. Resour. Environ. Econ.,* vol. 3, pp. 121-126, 12/31 2013.

[8] N. Tawfiq and D. A. Olsen, "Saudi Arabia's response to the 1991 Gulf oil spill," *Marine Pollution Bulletin,* vol. 27, pp. 333-345, 1993/01/01/ 1993.

[9] M. McNutt, S. Chu, J. Lubchenco, T. Hunter, G. Dreyfus, S. Murawski, *et al.*, "Applications of science and engineering to quantify and control the Deepwater Horizon oil spill," *Proceedings of the National Academy of Sciences,* vol. 109, pp. 20222-20228, 12/11 2012.

[10] A. Jernelöv, "The Threats from Oil Spills: Now, Then, and in the Future," *Ambio,* vol. 39, pp. 353-66, 07/01 2010.

[11] S. Libes, *Introduction to Marine Biogeochemistry*: Elsevier Science, 2011.

[12] G. Eglinton and R. J. Hamilton, "Leaf Epicuticular Waxes," *Science,* vol. 156, p. 1322, 1967.

[13] F. G. Prahl, J. T. Bennett, and R. Carpenter, "The early diagenesis of aliphatic hydrocarbons and organic matter in sedimentary particulates from Dabob Bay, Washington," *Geochimica et Cosmochimica Acta*, vol. 44, pp. 1967-1976, 1980/12/01/ 1980.

[14] M. Page, L. Nelson, M. Haverty, and G. Blomquist, "Cuticular hydrocarbons of eight species of north american cone beetles, Conophthorus hopkins," *Journal of chemical ecology*, vol. 16, pp. 1173-1198, 04/01 1990.

[15] M. Nishimura and E. W. Baker, "Possible origin of n-alkanes with a remarkable even-to-odd predominance in recent marine sediments," *Geochimica et Cosmochimica Acta*, vol. 50, pp. 299-305, 1986/02/01/ 1986.

[16] K. Hayakawa, N. Handa, N. Ikuta, and M. Fukuchi, "Downward fluxes of fatty acids and hydrocarbons during a phytoplankton bloom in the austral summer in Breid Bay, Antarctica," *Organic Geochemistry*, vol. 24, pp. 511-521, 1996/05/01/ 1996.

[17] C. H. Peterson, S. D. Rice, J. W. Short, D. Esler, J. L. Bodkin, B. E. Ballachey, *et al.*, "Long-Term Ecosystem Response to the Exxon Valdez Oil Spill," *Science*, vol. 302, p. 2082, 2003.

[18] M. Schratzberger, S. Neville, S. Painting, K. Weston, and L. Paltriguera, "Ecological and Socio-Economic Effects of Highly Protected Marine Areas (HPMAs) in Temperate Waters," *Frontiers in Marine Science*, vol. 6, 2019-December-13 2019.

[19] B. Bhushan, "Outlook: Bioinspired Hierarchical-Structured Surfaces for Green Science and Technology," ed, 2018, pp. 959-960.

[20] H. Furukawa, K. E. Cordova, M. O'Keeffe, and O. M. Yaghi, "The Chemistry and Applications of Metal-Organic Frameworks," *Science*, vol. 341, p. 1230444, 2013.

[21] X. Li, Y. Liu, J. Wang, J. Gascon, J. Li, and B. Van der Bruggen, "Metal–organic frameworks based membranes for liquid separation," *Chemical Society Reviews*, vol. 46, pp. 7124-7144, 2017.

[22] K.-Y. A. Lin, H. Yang, C. Petit, and F.-K. Hsu, "Removing oil droplets from water using a copper-based metal organic frameworks," *Chemical Engineering Journal*, vol. 249, pp. 293-301, 2014.

[23] Z. Abbasi, E. Shamsaei, X. Y. Fang, B. Ladewig, and H. Wang, "Simple fabrication of zeolitic imidazolate framework ZIF-8/polymer composite beads by phase inversion method for efficient oil sorption," *J Colloid Interface Sci,* vol. 493, pp. 150-161, May 1 2017.

[24] H. Zhu, Q. Zhang, B.-G. Li, and S. Zhu, "Engineering Elastic ZIF-8-Sponges for Oil-Water Separation," *Advanced Materials Interfaces,* vol. 4, p. 1700560, 2017.

[25] Y. Song, H. Li, M. Li, W. Li, Q. Yang, Y. Li, *et al.*, "Three dimensional MOF-sponge for fast dynamic adsorption," *Phys. Chem. Chem. Phys.*, vol. 19, 12/05 2016.

[26] Z. Kang, S. Wang, L. Fan, Z. Xiao, R. Wang, and D. Sun, "Surface wettability switching of metal-organic framework mesh for oil-water separation," *Materials Letters,* vol. 189, pp. 82-85, 2017/02/15/ 2017.

[27] K. Zhang, Q. Huo, Y.-Y. Zhou, H.-H. Wang, G.-P. Li, Y.-W. Wang, *et al.*, "Textiles/Metal–Organic Frameworks Composites as Flexible Air Filters for Efficient Particulate Matter Removal," *ACS Applied Materials & Interfaces,* vol. 11, pp. 17368-17374, 2019/05/15 2019.

[28] A. Sotto, G. Orcajo, J. M. Arsuaga, G. Calleja, and J. Landaburu-Aguirre, "Preparation and characterization of MOF-PES ultrafiltration membranes," *Journal of Applied Polymer Science,* vol. 132, 2015/06/05 2015.

[29] J. Song, W. Xu, and Y. Lu, "One-step electrochemical machining of superhydrophobic surfaces on aluminum substrates," *Journal of Materials Science,* vol. 47, pp. 162-168, 2012/01/01 2012.

[30] M. Ruan, W. Li, B. Wang, Q. Luo, F. Ma, and Z. Yu, "Optimal conditions for the preparation of superhydrophobic surfaces on al substrates using a simple etching approach," *Applied Surface Science,* vol. 258, pp. 7031-7035, 2012/07/01/ 2012.

[31] D. Zang, R. Zhu, W. Zhang, J. Wu, X. Yu, and Y. Zhang, "Stearic acid modified aluminum surfaces with controlled wetting properties and corrosion resistance," *Corrosion Science,* vol. 83, pp. 86-93, 2014/06/01/ 2014.

[32] H.-Y. Ryu, S. H. Yoon, D.-H. Han, H. Hafeez, N. R. Paluvai, C. S. Lee, *et al.*, "Fabrication of hydrophobic/hydrophilic switchable aluminum surface using poly(N-

isopropylacrylamide)," *Progress in Organic Coatings,* vol. 99, pp. 295-301, 2016/10/01/ 2016.

[33] S. Wang, Y. Song, and L. Jiang, "Microscale and nanoscale hierarchical structured mesh films with superhydrophobic and superoleophilic properties induced by long-chain fatty acids," *Nanotechnology,* vol. 18, p. 015103, 2006/12/08 2006.

[34] Z. Wei, D. Jiang, J. Chen, S. Ren, and L. Li, "Fabrication of mechanically robust superhydrophobic aluminum surface by acid etching and stearic acid modification," *Journal of Adhesion Science and Technology,* vol. 31, pp. 2380-2397, 2017/11/02 2017.

[35] X. Wu, L. Zheng, and D. Wu, "Fabrication of Superhydrophobic Surfaces from Microstructured ZnO-Based Surfaces via a Wet-Chemical Route," *Langmuir,* vol. 21, pp. 2665-2667, 2005/03/01 2005.

[36] Frances L. Heale, K. Page, J. S. Wixey, P. Taylor, I. P. Parkin, and C. J. Carmalt, "Inexpensive and non-toxic water repellent coatings comprising SiO2 nanoparticles and long chain fatty acids," *RSC Advances,* vol. 8, pp. 27064-27072, 2018.

[37] R. Gupta, G. Dunderdale, M. England, and A. Hozumi, "Oil/water separation techniques: A review of recent progresses and future directions," *J. Mater. Chem. A,* vol. 5, 05/05 2017.

[38] G. Wang, Z. Zeng, X. Wu, T. Ren, J. Han, and Q. Xue, "Three-dimensional structured sponge with high oil wettability for the clean-up of oil contaminations and separation of oil–water mixtures," *Polymer Chemistry,* vol. 5, pp. 5942-5948, 2014.

[39] J. Yong, J. Huo, F. Chen, Q. Yang, and X. Hou, "Oil/water separation based on natural materials with super-wettability: recent advances," *Physical Chemistry Chemical Physics,* vol. 20, pp. 25140-25163, 2018.

[40] Y. Lu and W. Yuan, "Superhydrophobic three-dimensional porous ethyl cellulose absorbent with micro/nano-scale hierarchical structures for highly efficient removal of oily contaminants from water," *Carbohydrate Polymers,* vol. 191, 03/01 2018.

[41] S. Eom, D. W. Kang, M. Kang, J. Choe, H. Kim, D. Kim, *et al.*, "Fine-tuning of wettability in a single metal-organic framework: Via postcoordination modification and

its reduced graphene oxide aerogel for oil-water separation," *Chemical Science*, vol. 10, 01/16 2019.

[42] D. Wu, Z. Yu, W. Wu, L. Fang, and H. Zhu, "Continuous oil–water separation with surface modified sponge for cleanup of oil spills," *RSC Advances*, vol. 4, pp. 53514-53519, 2014.

[43] Y. Guan, F. Cheng, and Z. Pan, "Superwetting Polymeric Three Dimensional (3D) Porous Materials for Oil/Water Separation: A Review," *Polymers*, vol. 11, p. 806, 2019.

[44] C. C. Azubuike, C. B. Chikere, and G. C. Okpokwasili, "Bioremediation techniques–classification based on site of application: principles, advantages, limitations and prospects," *World Journal of Microbiology and Biotechnology*, vol. 32, p. 180, 2016/09/16 2016.

[45] F. Attiogbe, M. Glover-Amengor, and K. Nyadziehe, "Correlating Biochemical and Chemical Oxygen Demand of Effluents - A Case Study of Selected Industries in Kumasi, Ghana," *West African Journal of Applied Ecology*, vol. 11, 09/07 2009.

[46] E. Obi, F. Kamgba, and D. Obi, "Techniques of Oil Spill Response in the sea," *IOSR Journal of Applied Physics*, vol. 6, 11/30 2013.

[47] G. Ren, Y. Song, X. Li, Y. Zhou, Z. Zhang, and X. Zhu, "A superhydrophobic copper mesh as an advanced platform for oil-water separation," *Applied Surface Science*, vol. 428, pp. 520-525, 2018/01/15/ 2018.

[48] G. Wang, L. He, Y. Lu, and Z. Chen, "Study on oil-water separating behavior of gravity separator," vol. 27, pp. 112-115, 11/01 2006.

[49] J. Saththasivam, K. Loganathan, and S. Sarp, "An overview of oil–water separation using gas flotation systems," *Chemosphere*, vol. 144, pp. 671-680, 2016/02/01/ 2016.

[50] Z. Xue, Y. Cao, N. Liu, L. Feng, and L. Jiang, "Special wettable materials for oil/water separation," *Journal of Materials Chemistry A*, vol. 2, pp. 2445-2460, 2014.

[51] R. S. Jackson, "8 - Postfermentation Treatments and Related Topics," in *Wine Science (Third Edition)*, R. S. Jackson, Ed., ed San Diego: Academic Press, 2008, pp. 418-519.

[52] M. Fingas and J. Banta, *Review of literature related to oil spill dispersants*, 2009.

[53] M. Adebajo, R. Frost, T. Kloprogge, O. Carmody, and S. Kokot, "Porous Materials for Oil Spill Cleanup: A Review of Synthesis and Absorbing Properties," *Journal of Porous Materials,* vol. 10, pp. 159-170, 09/01 2003.

[54] A. A. Allen and R. J. Ferek, *Advantages and disadvantages of burning spilled oil*. United States: American Petroleum Institute, 1993.

[55] L. Bandura, A. Woszuk, and D. Kołodyńska, "Application of mineral sorbents for petroleum substances removal: A review," *Minerals,* vol. 7, 03/04 2017.

[56] D. D. Nguyen, N.-H. Tai, S.-B. Lee, and W.-S. Kuo, "Superhydrophobic and superoleophilic properties of graphene-based sponges fabricated using a facile dip coating method," *Energy & Environmental Science,* vol. 5, pp. 7908-7912, 2012.

[57] S. Qiu, Y. Li, G. Li, Z. Zhang, Y. Li, and T. Wu, "Robust Superhydrophobic Sepiolite-Coated Polyurethane Sponge for Highly Efficient and Recyclable Oil Absorption," *ACS Sustainable Chemistry & Engineering,* vol. 7, pp. 5560-5567, 2019/03/04 2019.

[58] S. Qiu, B. Jiang, X. Zheng, J. Zheng, C. Zhu, and M. Wu, "Hydrophobic and fire-resistant carbon monolith from melamine sponge: A recyclable sorbent for oil–water separation," *Carbon,* vol. 84, pp. 551-559, 2015/04/01/ 2015.

[59] L. Yan, Y. Zhao, F. Zha, Q. T. Wang, and Z. Lei, "Correction: One-step fabrication of robust fabrics with both-faced superhydrophobicity for the separation and capture of oil from water," *Physical chemistry chemical physics : PCCP,* vol. 17, 02/06 2015.

[60] P. Calcagnile, D. Fragouli, I. S. Bayer, G. C. Anyfantis, L. Martiradonna, P. D. Cozzoli, *et al.*, "Magnetically Driven Floating Foams for the Removal of Oil Contaminants from Water," *ACS Nano,* vol. 6, pp. 5413-5419, 2012/06/26 2012.

[61] C. R. Crick, J. A. Gibbins, and I. P. Parkin, "Superhydrophobic polymer-coated copper-mesh; membranes for highly efficient oil–water separation," *Journal of Materials Chemistry A,* vol. 1, pp. 5943-5948, 2013.

[62] M. Padaki, R. Surya Murali, M. S. Abdullah, N. Misdan, A. Moslehyani, M. A. Kassim, *et al.*, "Membrane technology enhancement in oil–water separation. A review," *Desalination,* vol. 357, pp. 197-207, 2015/02/02/ 2015.

[63] J. K. Haken, "SYNTHETIC POLYMERS | Gas Chromatography," in *Encyclopedia of Separation Science*, I. D. Wilson, Ed., ed Oxford: Academic Press, 2000, pp. 4334-4343.

[64] L. Verdolotti, M. R. Di Caprio, M. Lavorgna, and G. G. Buonocore, "Chapter 9 - Polyurethane Nanocomposite Foams: Correlation Between Nanofillers, Porous Morphology, and Structural and Functional Properties," in *Polyurethane Polymers*, S. Thomas, J. Datta, J. T. Haponiuk, and A. Reghunadhan, Eds., ed Amsterdam: Elsevier, 2017, pp. 277-310.

[65] Y.-R. Lee, M.-S. Jang, H.-Y. Cho, H.-J. Kwon, S. Kim, and W.-S. Ahn, "ZIF-8: A comparison of synthesis methods," *Chemical Engineering Journal,* vol. 271, pp. 276-280, 2015/07/01/ 2015.

[66] O. Yaghi, M. Kalmutzki, and C. Diercks, "Zeolitic Imidazolate Frameworks," ed, 2019, pp. 463-479.

[67] D. Zou, D. Liu, and J. Zhang, "From Zeolitic Imidazolate Framework-8 to Metal-Organic Frameworks (MOFs): Representative Substance for the General Study of Pioneering MOF Applications," *ENERGY & ENVIRONMENTAL MATERIALS,* vol. 1, pp. 209-220, 2018/12/01 2018.

[68] P. Hiremath, K. Nuguru, and V. Agrahari, "Chapter 8 - Material Attributes and Their Impact on Wet Granulation Process Performance," in *Handbook of Pharmaceutical Wet Granulation*, A. S. Narang and S. I. F. Badawy, Eds., ed: Academic Press, 2019, pp. 263-315.

[69] T.-H. Chen, I. Popov, O. Zenasni, O. Daugulis, and O. Š. Miljanić, "Superhydrophobic perfluorinated metal–organic frameworks," *Chemical Communications,* vol. 49, pp. 6846-6848, 2013.

[70] E. E. Sann, Y. Pan, Z. Gao, S. Zhan, and F. Xia, "Highly hydrophobic ZIF-8 particles and application for oil-water separation," *Separation and Purification Technology,* vol. 206, pp. 186-191, 2018.

[71] S. Chowdhury, "Advancement of Oil/Water Separating Materials: Merits and Demerits in Real-Time Applications," *MOJ Polymer Science,* vol. 1, 03/17 2017.

[72] Y. Cai, D. Chen, N. Li, Q. Xu, H. Li, J. He, *et al.*, "Nanofibrous metal–organic framework composite membrane for selective efficient oil/water emulsion separation," *Journal of Membrane Science,* vol. 543, pp. 10-17, 2017/12/01/ 2017.

[73] G. Xiaojia, X. Wang, X. Ouyang, and C. Wen, "Flexible Superhydrophobic and Superoleophilic MoS2 Sponge for Highly Efficient Oil-Water Separation," *Scientific Reports,* vol. 6, p. 27207, 06/02 2016.

[74] T. Liu, G. Zhao, W. Zhang, H. Chi, C. Hou, and Y. Sun, "The preparation of superhydrophobic graphene/melamine composite sponge applied in treatment of oil pollution," *Journal of Porous Materials,* vol. 22, 08/09 2015.

[75] K. Jayaramulu, K. K. R. Datta, C. Rösler, M. Petr, M. Otyepka, R. Zboril, *et al.*, "Biomimetic Superhydrophobic/Superoleophilic Highly Fluorinated Graphene Oxide and ZIF-8 Composites for Oil-Water Separation," *Angewandte Chemie International Edition,* vol. 55, pp. 1178-1182, 2016.

[76] D. D. Nguyen, N.-H. Tai, S.-B. Lee, and W.-S. Kuo, "Superhydrophobic and superoleophilic properties of graphene-based sponges fabricated using a facile dip coating method," *Energy & Environmental Science,* vol. 5, p. 7908, 2012.

[77] Y. Liu, J. Ma, T. Wu, X. Wang, G. Huang, Y. Liu, *et al.*, "Cost-Effective Reduced Graphene Oxide-Coated Polyurethane Sponge As a Highly Efficient and Reusable Oil-Absorbent," *ACS Applied Materials & Interfaces,* vol. 5, pp. 10018-10026, 2013/10/23 2013.

[78] B. Ge, Z. Zhang, X. Zhu, X. Men, and X. Zhou, "A superhydrophobic/superoleophilic sponge for the selective absorption oil pollutants from water," *Colloids and Surfaces A: Physicochemical and Engineering Aspects,* vol. 457, pp. 397-401, 2014.

[79] Z. Xu, J. Wang, H. Li, and Y. Wang, "Coating sponge with multifunctional and porous metal-organic framework for oil spill remediation," *Chemical Engineering Journal,* vol. 370, pp. 1181-1187, 2019.

[80] Z. Lei, Y. Deng, and C. Wang, "Multiphase surface growth of hydrophobic ZIF-8 on melamine sponge for excellent oil/water separation and effective catalysis in a Knoevenagel reaction," *Journal of Materials Chemistry A*, vol. 6, pp. 3258-3263, 2018.

[81] Y. Zhang, N. Zhang, S. Zhou, X. Lv, C. Yang, W. Chen, *et al.*, "Facile Preparation of ZIF-67 Coated Melamine Sponge for Efficient Oil/Water Separation," *Industrial & Engineering Chemistry Research*, vol. 58, pp. 17380-17388, 2019.

[82] X. Zhang, J. Li, G. Wang, F. Fu, X. Gao, F. Niu, *et al.*, "Preparation of Superhydrophobic Magnetic Polyurethane Sponge for Removing Oil Pollutants from Water," *IOP Conference Series: Materials Science and Engineering*, vol. 392, p. 042003, 08/02 2018.

[83] V.-H. T. Tran and B.-K. Lee, "Novel fabrication of a robust superhydrophobic PU@ZnO@Fe3O4@SA sponge and its application in oil-water separations," *Scientific Reports*, vol. 7, p. 17520, 2017/12/13 2017.

[84] L. Dashairya, A. Sahu, and P. Saha, "Stearic acid treated polypyrrole-encapsulated melamine formaldehyde superhydrophobic sponge for oil recovery," *Advanced Composites and Hybrid Materials*, vol. 2, pp. 70-82, 2019/03/01 2019.

[85] P. Jiang, K. Li, X. Chen, R. Dan, and Y. Yu, "Magnetic and Hydrophobic Composite Polyurethane Sponge for Oil–Water Separation," *Applied Sciences*, vol. 10, p. 1453, 02/21 2020.

[86] M. Shi, R. Huang, W. Qi, R. Su, and Z. He, "Synthesis of superhydrophobic and high stable Zr-MOFs for oil-water separation," *Colloids and Surfaces A: Physicochemical and Engineering Aspects*, p. 125102, 2020/05/31/ 2020.

[87] M. M. Ghobashy and Z. I. Abdeen, "Radiation Crosslinking of Polyurethanes: Characterization by FTIR, TGA, SEM, XRD, and Raman Spectroscopy," *Journal of Polymers*, vol. 2016, pp. 1-9, 2016.

[88] N. A. H. Md. Nordin, A. Ismail, N. Misdan, and N. Nazri, *Modified ZIF-8 mixed matrix membrane for CO2/CH4 separation* vol. 1891, 2017.

[89] M. A. Alaa, K. Yusoh, and S. F. Hasany, "Pure Polyurethane and Castor Oil Based Polyurethane: Synthesis and Characterization," *Journal of Mechanical Engineering and Sciences*, vol. 8, pp. 1507-1515, 2015.

[90] J. Wang and Y. Zheng, "Oil/water mixtures and emulsions separation of stearic acid-functionalized sponge fabricated via a facile one-step coating method," *Separation and Purification Technology*, vol. 181, pp. 183-191, 2017/06/30/ 2017.

[91] Z. Zhen, T. F. Xi, and Y. F. Zheng, "Surface modification by natural biopolymer coatings on magnesium alloys for biomedical applications," pp. 301-333, 2015.

[92] D. Wu, W. Wu, Z. Yu, C. Zhang, and H. Zhu, "Facile Preparation and Characterization of Modified Polyurethane Sponge for Oil Absorption," *Industrial & Engineering Chemistry Research*, vol. 53, pp. 20139-20144, 2014.

[93] Y. Liu, J. Ma, T. Wu, X. Wang, G. Huang, Y. Liu, *et al.*, "Cost-effective reduced graphene oxide-coated polyurethane sponge as a highly efficient and reusable oil-absorbent," *ACS Appl Mater Interfaces*, vol. 5, pp. 10018-26, Oct 23 2013.

[94] C. Wu, Q. Liu, R. Chen, J. Liu, H. Zhang, R. Li, *et al.*, "Fabrication of ZIF-8@SiO2 Micro/Nano Hierarchical Superhydrophobic Surface on AZ31 Magnesium Alloy with Impressive Corrosion Resistance and Abrasion Resistance," *ACS Appl Mater Interfaces*, vol. 9, pp. 11106-11115, Mar 29 2017.

[95] Y. Zhang, Y. Jia, and L. a. Hou, "Synthesis of zeolitic imidazolate framework-8 on polyester fiber for PM2.5 removal," *RSC Advances*, vol. 8, pp. 31471-31477, 2018.

[96] H. Huang, M. Tian, J. Yang, H. Li, W. Liang, L. Zhang, *et al.*, "Stearic acid surface modifying Mg(OH)2: Mechanism and its effect on properties of ethylene vinyl acetate/Mg(OH)2 composites," *Journal of Applied Polymer Science*, vol. 107, pp. 3325-3331, 03/05 2008.

[97] S. Salehabadi, J. Seyfi, I. Hejazi, S. M. Davachi, A. H. Naeini, and M. Khakbaz, "Nanosilica-decorated sponges for efficient oil/water separation: role of nanoparticle's type and concentration," *Journal of Materials Science*, vol. 52, pp. 7017-7027, 2017.

[98] J. Wang and Y. Zheng, "Oil/water mixtures and emulsions separation of stearic acid-functionalized sponge fabricated via a facile one-step coating method," *Separation and Purification Technology*, vol. 181, 03/01 2017.